

The emerging role of artificial intelligence in internal radiation dosimetry

Habib Zaidi^{1,2,3}

15th EURADOS School, Belgrade, 23 June 2022



¹Geneva University Hospital, Geneva, Switzerland

²University of Groningen, Groningen, Netherlands

³University of Southern Denmark, Odense, Denmark

Email: habib.zaidi@hcuge.ch

Web: <http://www.pinlab.ch>



SINFONIA - Medical radiation risk appraisal



European
Commission

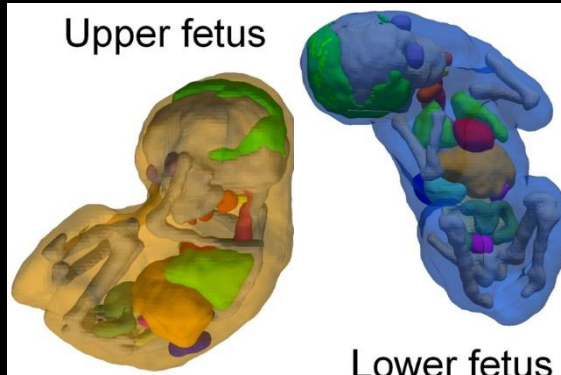
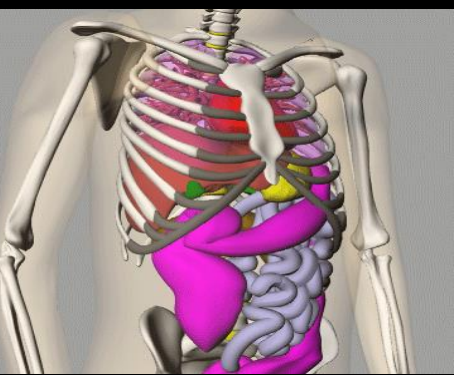
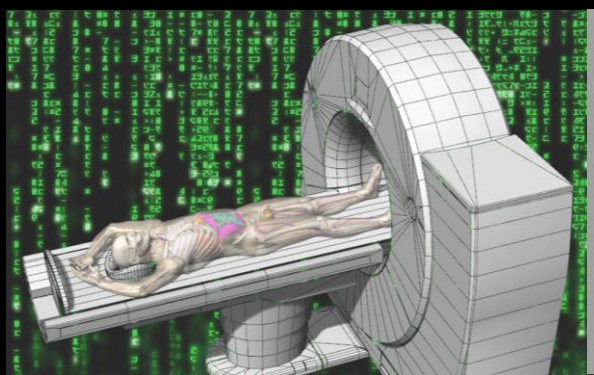
Horizon 2020
European Union funding
for Research & Innovation



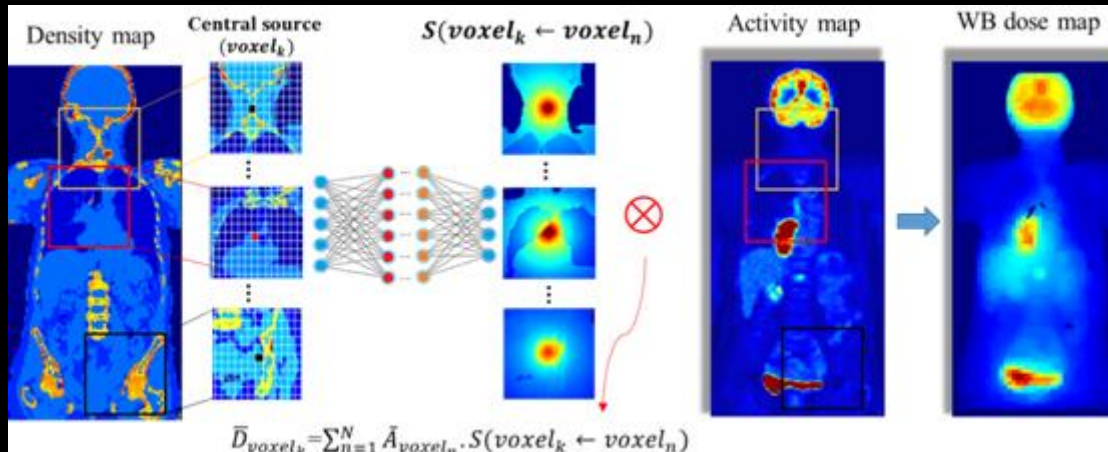
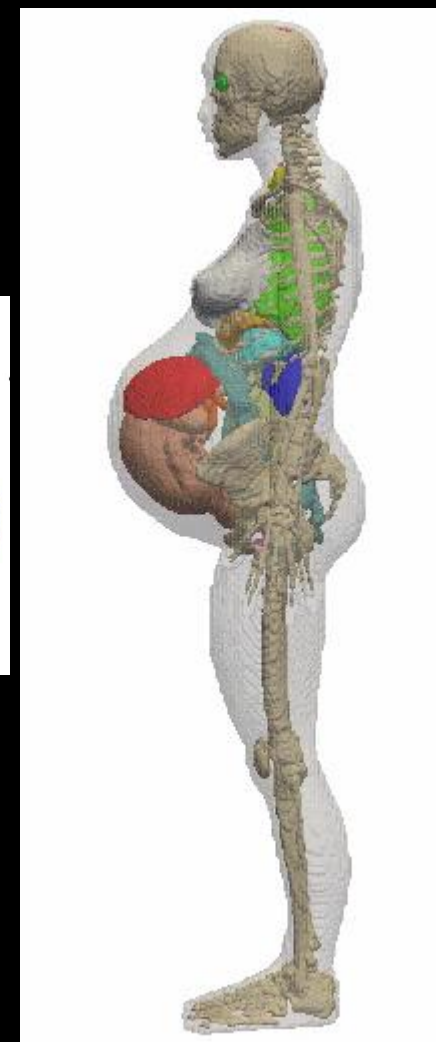
EEC H2020 (2020-2024) <https://www.sinfonia-appraisal.eu/>

«Radiation risk appraisal for detrimental effects from medical exposure
during management of patients with lymphoma or brain tumours»

NFRP-945196 SINFONIA (5'999'999 €)



38w-gestation



Outline

- Advances in multimodality molecular imaging
- Why do we need AI in radiation dosimetry?
- Promise of AI in internal radiation dosimetry
 - ➡ Low-dose CT/**PET/SPECT** imaging (chest/**brain/WB/cardiac**)
 - ➡ Medical image segmentation (CT and **PET**)
 - ➡ Cross-modality image conversion (**MRI**→CT)
 - ➡ Quantification (attenuation & scatter correction in PET)
 - ➡ Computational modeling and radiation dosimetry
 - ➡ Prognostic modeling and outcome prediction
- Summary and future perspectives

Recent SPECT/CT scanner designs (CZT)



D-SPECT(Spectrum Dynamics)

Discovery 870 CZT (GE)



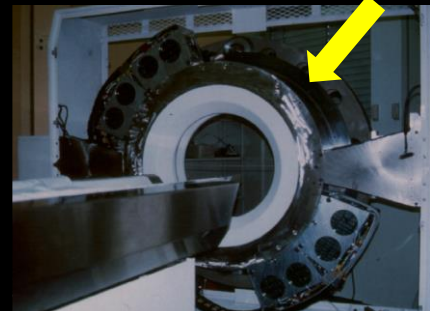
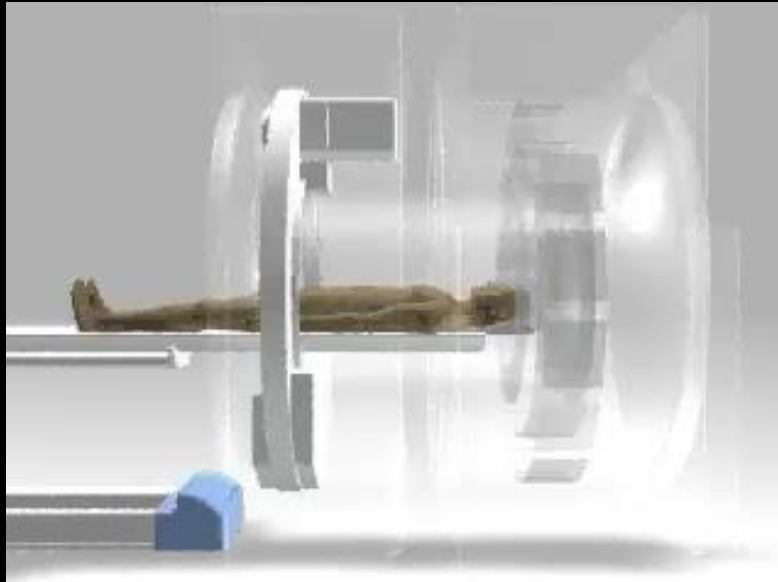
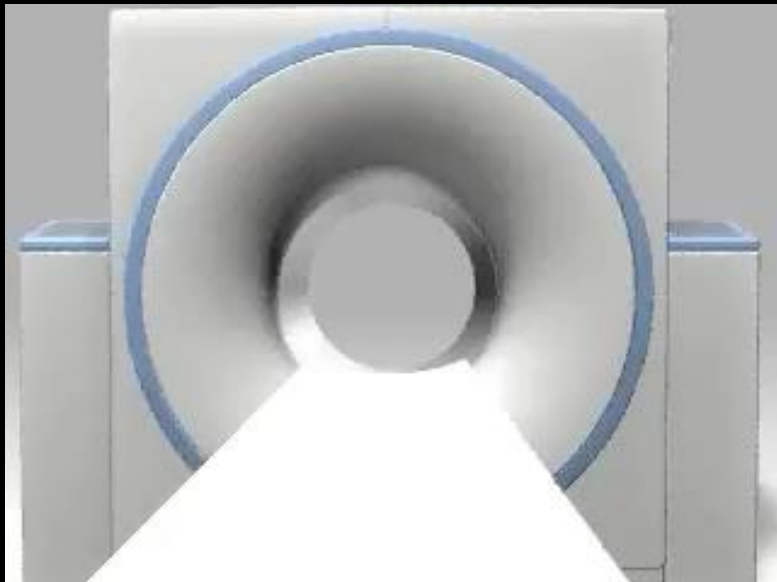
VERITON-CT (Spectrum Dynamics)



StarGuide (GE)

Veriton-CT SPECT/CT camera

Principles of PET/CT



Scout



Spiral CT



PET

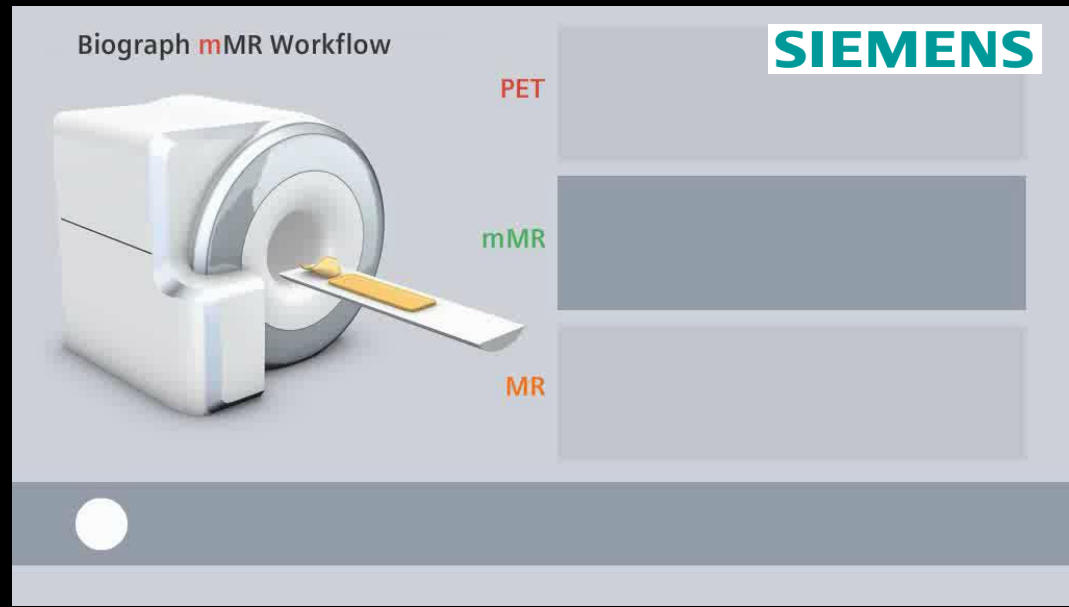


PET/CT





Biograph mMR



SIEMENS



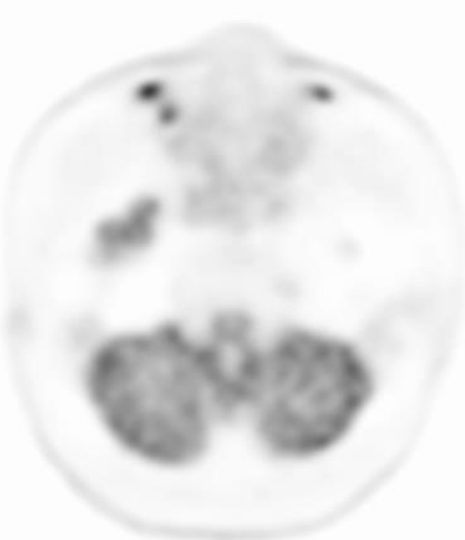
uPMR 790 HD TOF PET/MR

UNITED IMAGING

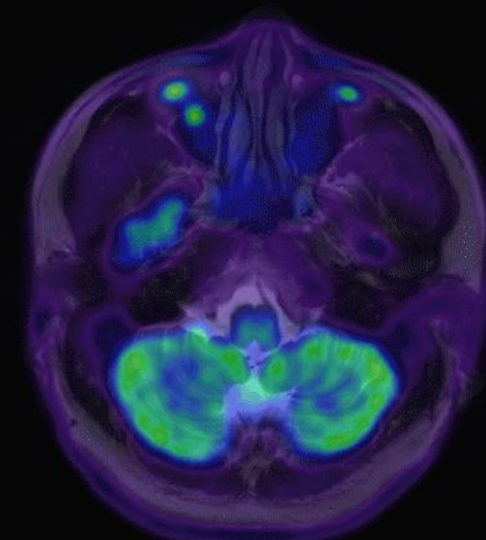
Clinical applications of PET/MRI



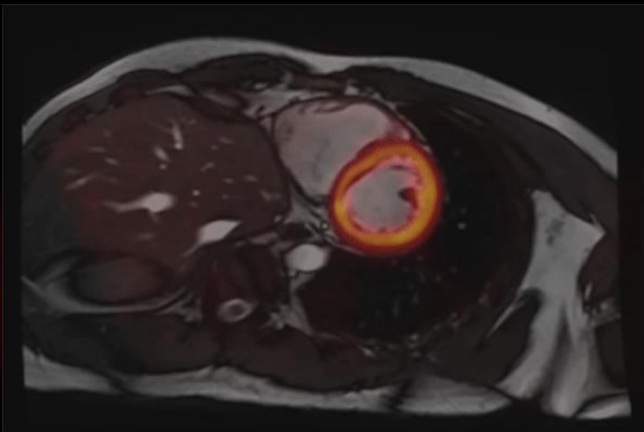
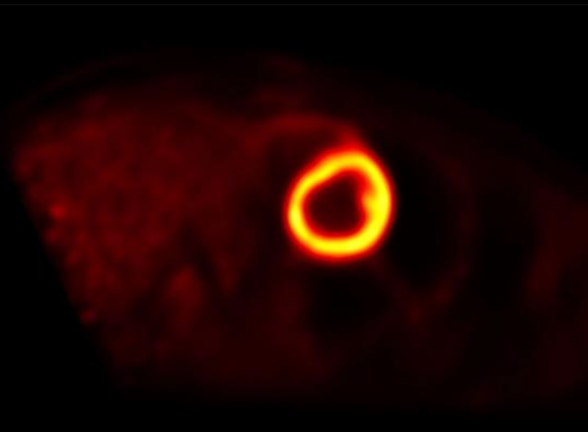
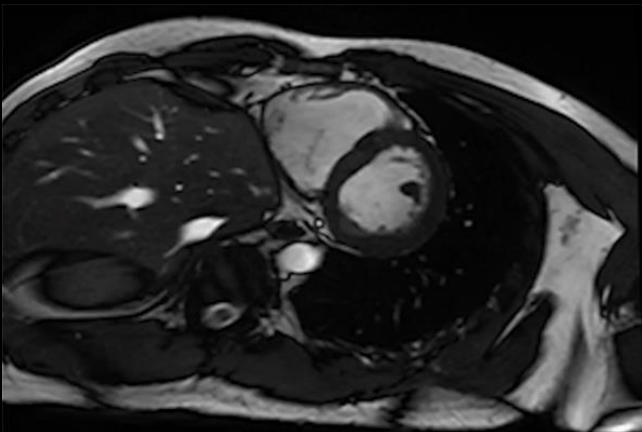
MRI

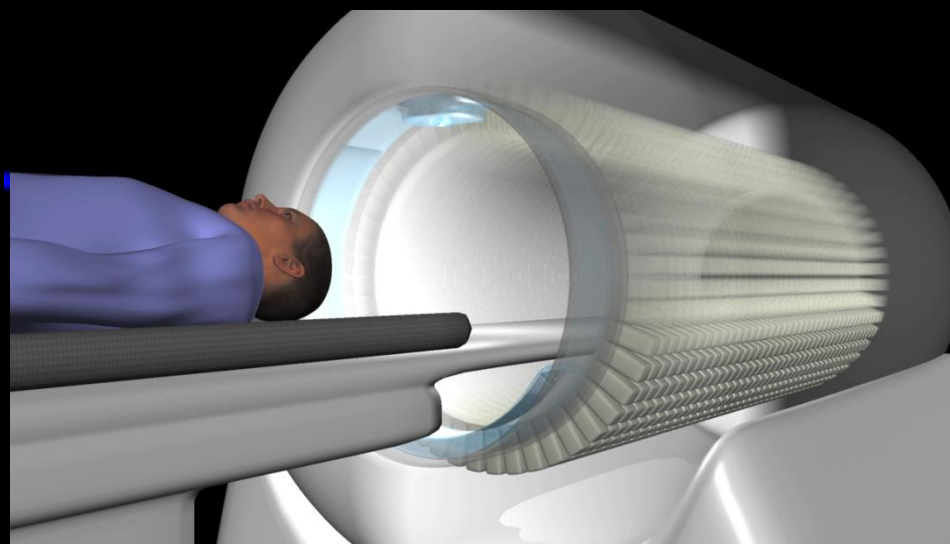
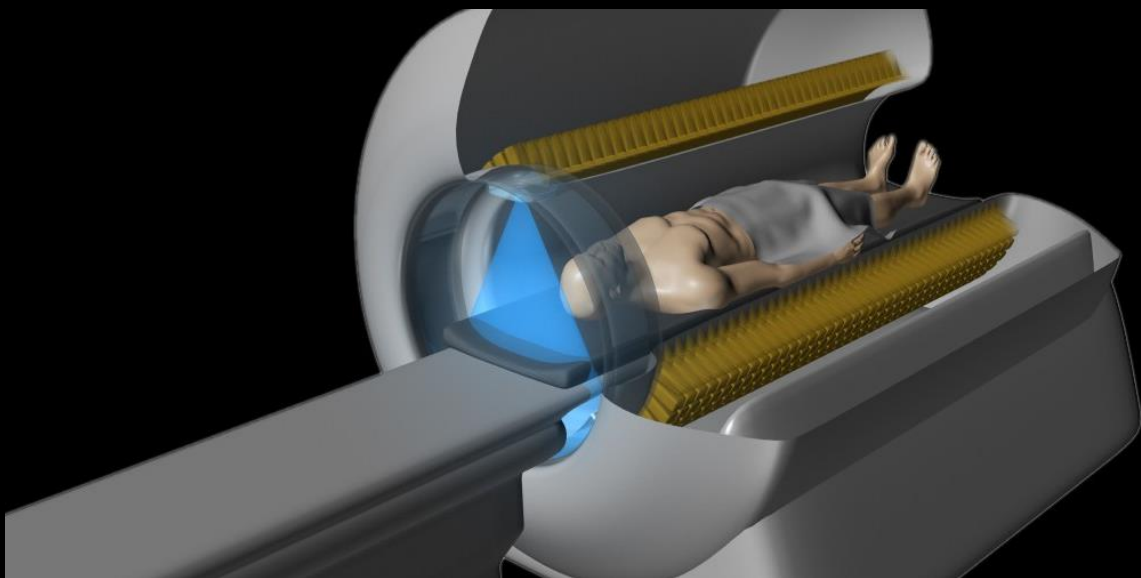


PET



PET-MRI





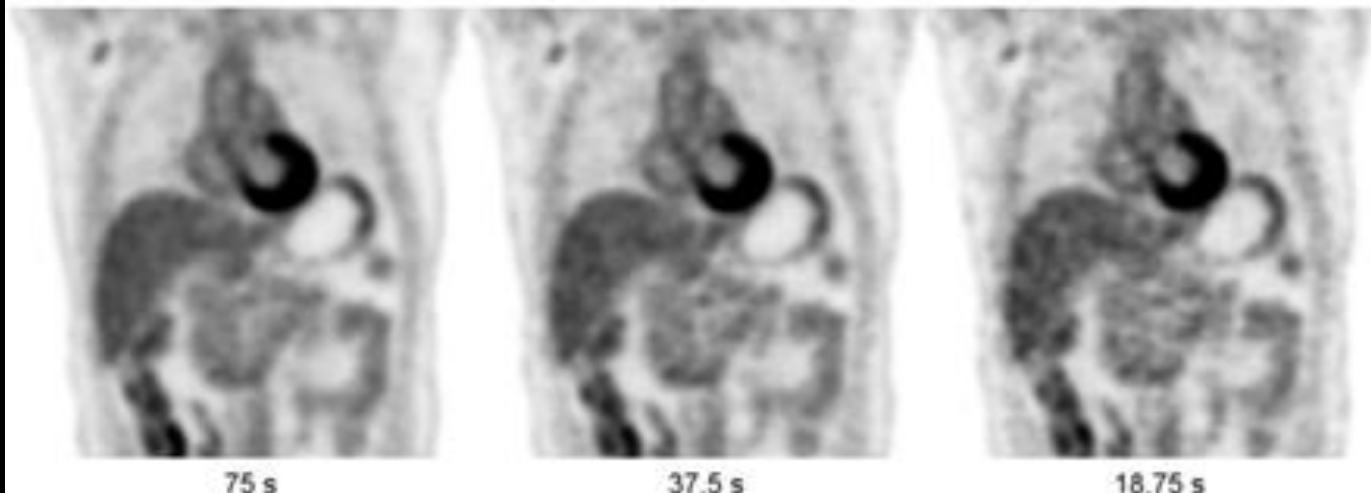
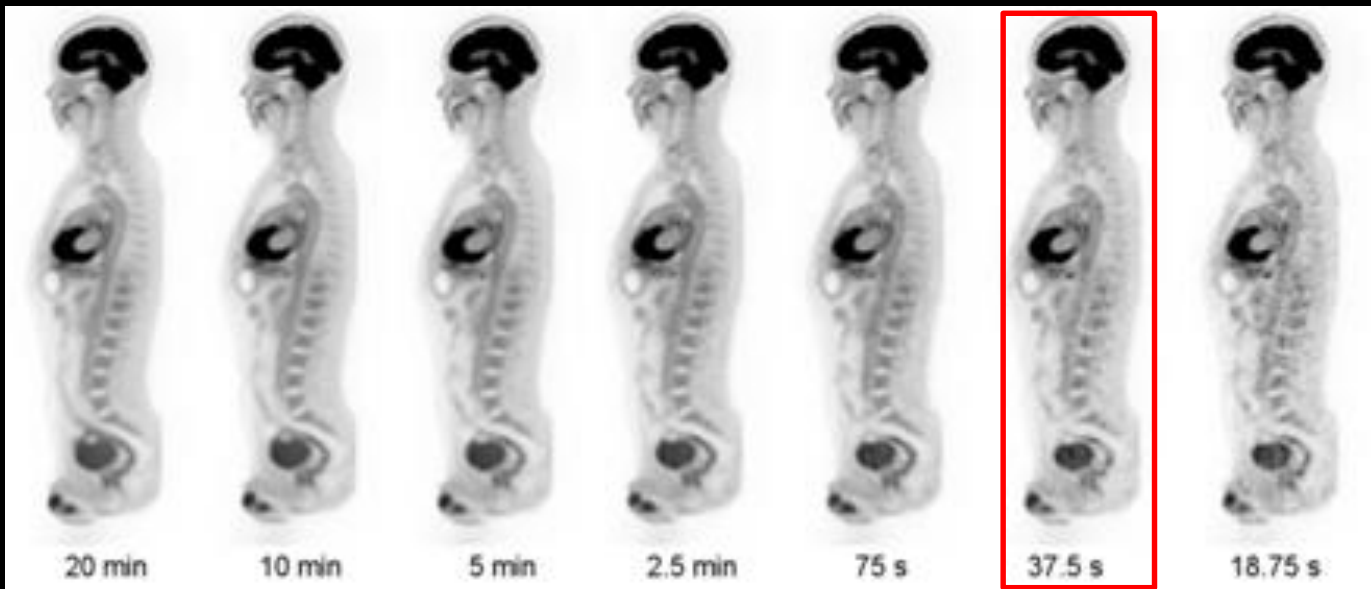
Penn PET



Quadra
106 cm AFOV
230 ps TOF CTR



Total-body PET: Towards systemic medicine



75 s

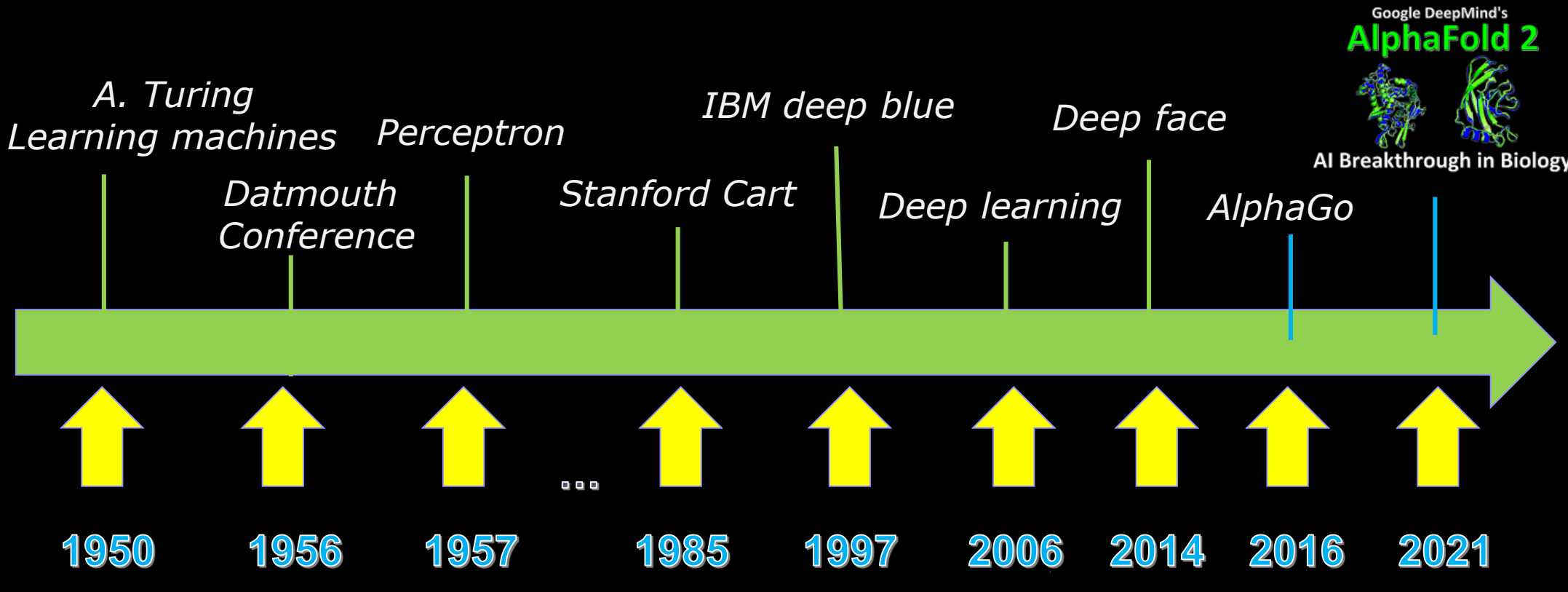
37.5 s

18.75 s

290 MBq injected, 82 min uptake

Novel detector concepts: Multifunctional PET

Artificial intelligence in medical physics





Contents lists available at ScienceDirect

Physica Medica

journal homepage: www.elsevier.com/locate/ejmp



POINT/COUNTERPOINT

Suggestions for topics suitable for these Point/Counterpoint debates should be addressed to Habib Zaidi, Geneva University Hospital, Geneva, Switzerland: habib.zaidi@hcuge.ch; Jing Cai, The Hong Kong Polytechnic University, Hong Kong: jing.cai@polyu.edu.hk; and/or Gerald White, Colorado Associates in Medical Physics: gerald.white@mindspring.com. Persons participating in Point/Counterpoint discussions are selected for their knowledge and communicative skill. Their positions for or against a proposition may or may not reflect their personal opinions or the positions of their employers.

Artificial intelligence should be part of medical physics graduate program curriculum

Lei Xing, Ph.D.^{a)}

*Department of Radiation Oncology, Stanford University, Stanford, CA 94305, USA,
(Tel: 650-498-7896; E-mail: lei@stanford.edu)*

Steven Goetsch, Ph.D.^{a)}

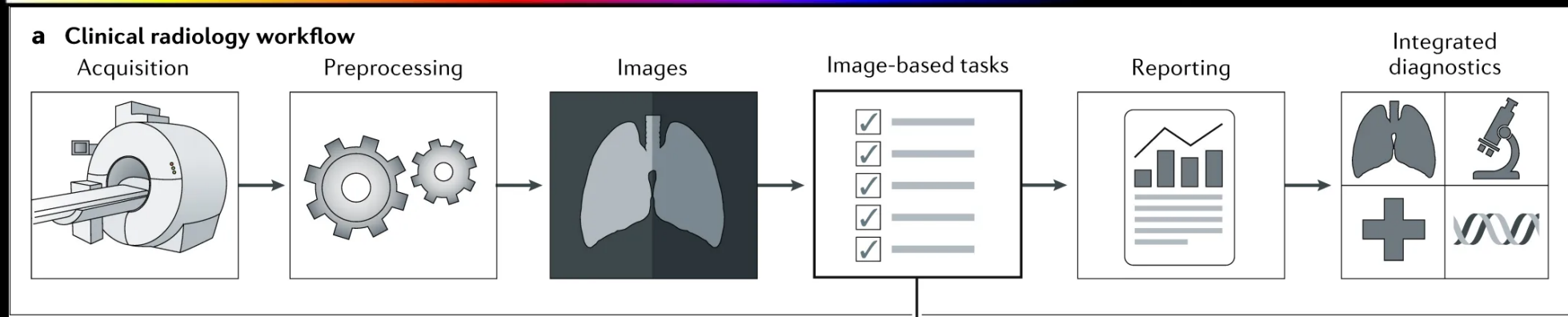
*San Diego Gamma Knife Center, La Jolla, CA 92037, USA,
(Tel: 858-794-8847; E-mail: steven@sdradiotherapy.com)*

Jing Cai, Ph.D., Moderator

*(Received 27 October 2020; revised 27 October 2020; accepted for publication 1 November 2020;
published 11 April 2021)*

[<https://doi.org/10.1002/mp.14587>]

Artificial intelligence impacting radiology

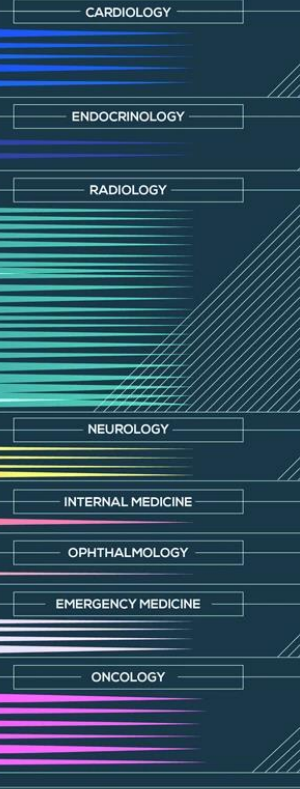


FDA-approved AI medical devices/algorithms

FDA APPROVALS FOR ARTIFICIAL INTELLIGENCE-BASED DEVICES IN MEDICINE

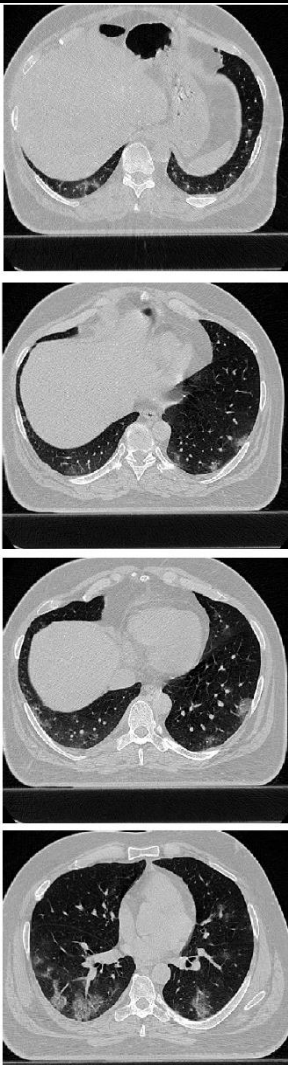
2016.11.	Arterys Cardio DL	software analyzing cardiovascular images from MR
2017.03.	EnsoSleep	diagnosis of sleep disorders
2017.11.	Arterys Oncology DL	medical diagnostic application
2018.01.	Idx	detection of diabetic retinopathy
2018.02.	ContaCT	stroke detection on CT
	OsteoDetect	X-ray wrist fracture diagnosis
2018.03.	Guardian Connect System	predicting blood glucose changes
2018.05.	EchoMD (AEF Software)	echocardiogram analysis
2018.06.	DreaMed	managing Type 1 diabetes.
2018.07.	BriefCase	triage and diagnosis of time sensitive patients
	ProFound™ AI Software V2.1	breast density via mammography
2018.08.	Arterys MICA	liver and lung cancer diagnosis on CT and MRI
2018.09.	SubtlePET	radiology image processing software
	AI-ECG Platform	ECG analysis support
2018.10.	AccipioRx	acute intracranial hemorrhage triage algorithm
	icobrain	MRI brain interpretation
2018.11.	FerriSmart Analysis System	measure liver iron concentration
2019.03.	cmTriage	mammogram workflow
2019.04.	Deep Learning Image Reconstruction	CT image reconstruction
2019.05.	HealthPNX	chest X-Ray assessment pneumothorax
2019.06.	Advanced Intelligent Clear-IQ Engine	noise reduction algorithm
2019.07.	SubtleMR	radiology image processing software
	AI-Rad Companion (Pulmonary)	CT image reconstruction - pulmonary
2019.08.	Critical Care Suite	chest X-Ray assessment pneumothorax
2019.09.	AI-Rad Companion (Cardiovascular)	CT image reconstruction - cardiovascular
2019.11.	EchoGo Core	quantification and reporting of results of cardiovascular function
2019.12.	TransparaTM	mammogram workflow
2020.01.	QuantX	radiological software for lesions suspicious for cancer
	Eko Analysis Software	cardiac Monitor

TYPE OF FDA APPROVAL
510(K) PREMARKET NOTIFICATION
DE NOVO PATHWAY
PMA

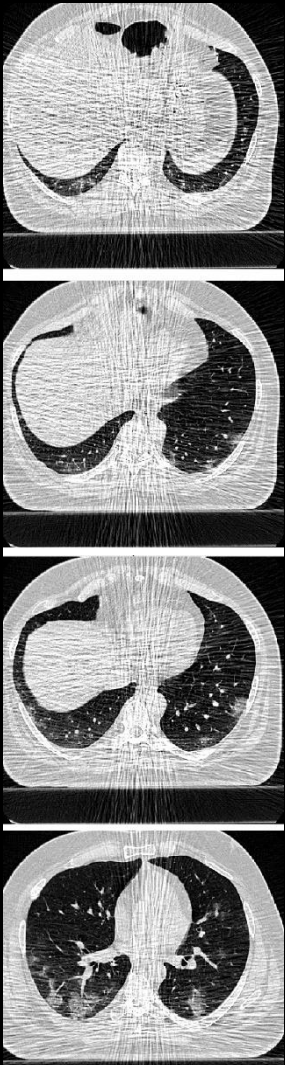


Deep learning-guided low-dose CT imaging

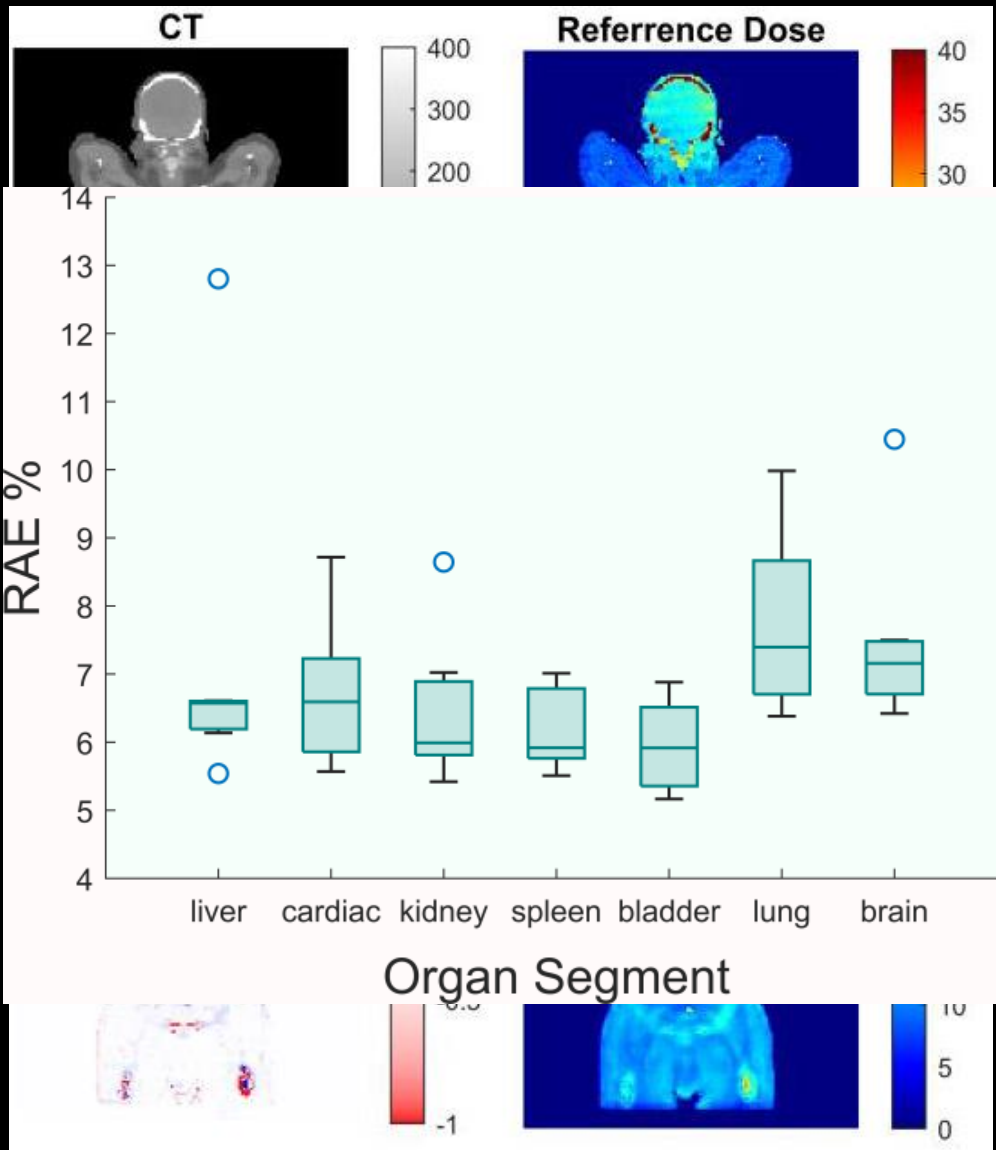
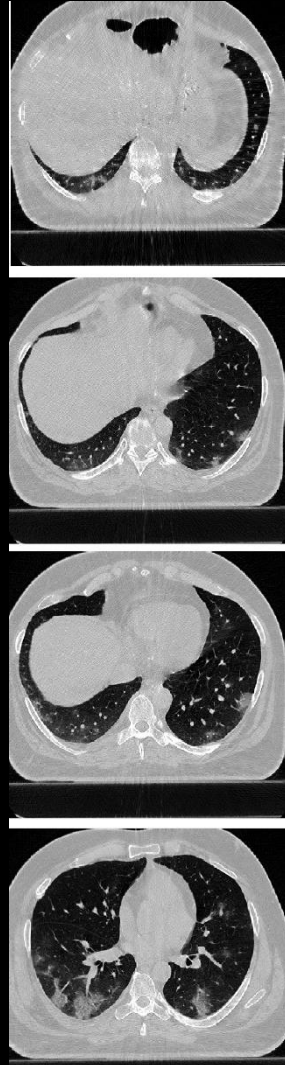
Full-dose



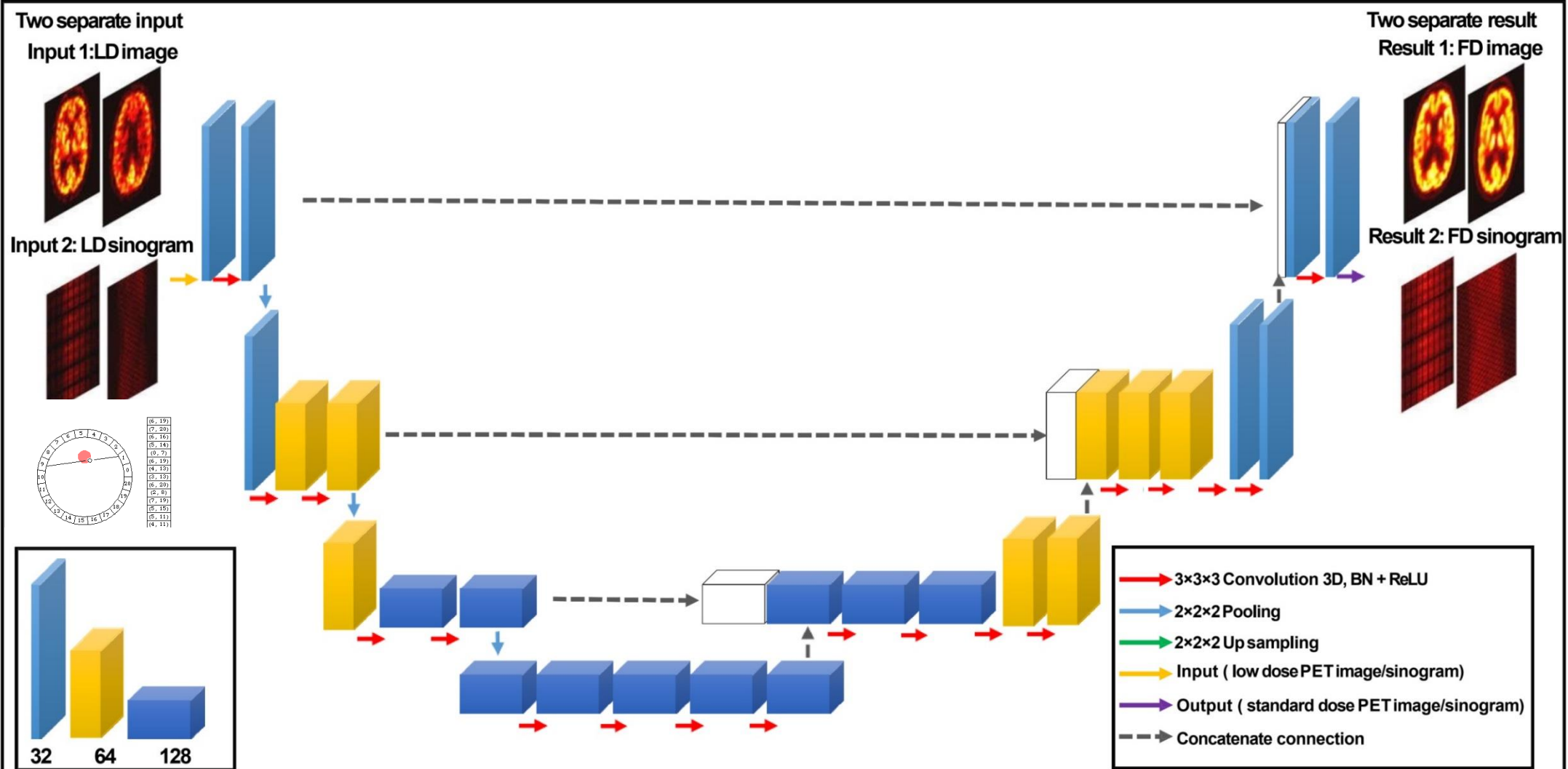
Low-dose



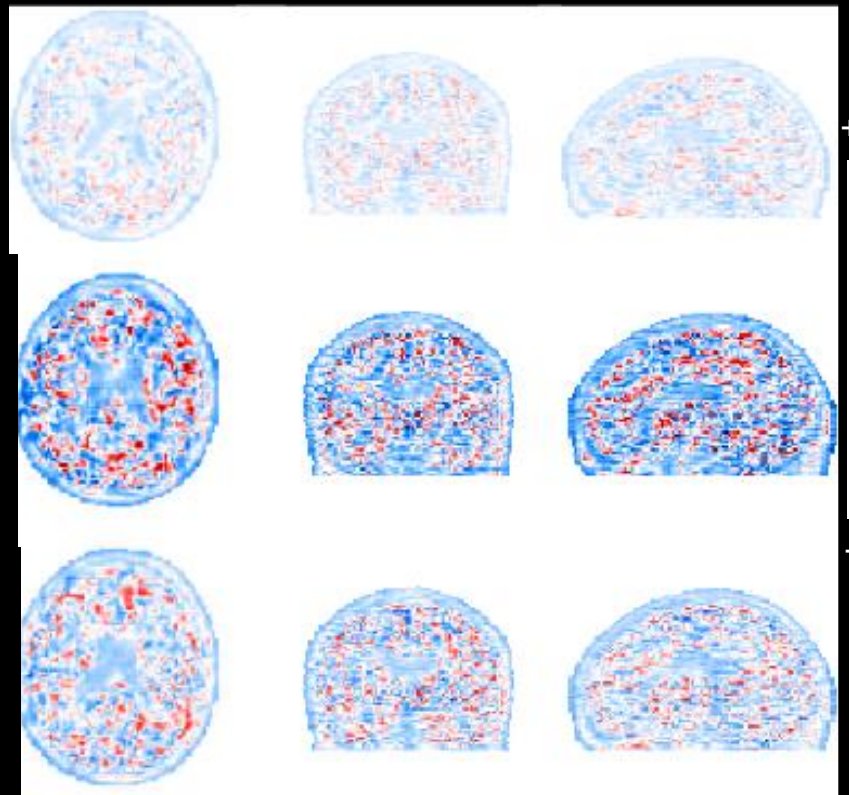
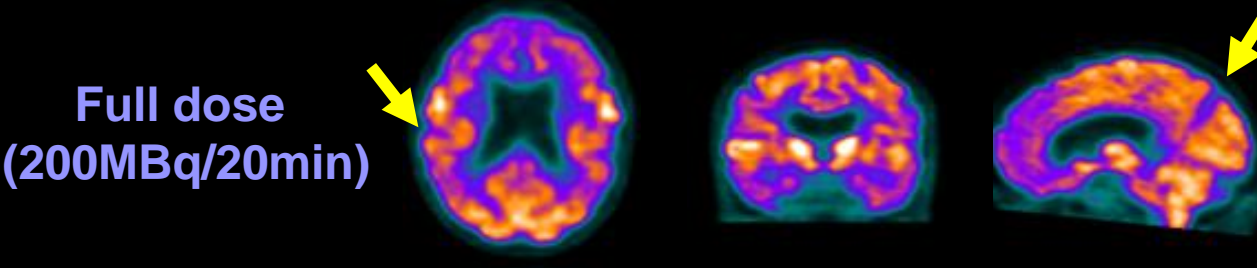
Predicted full-dose



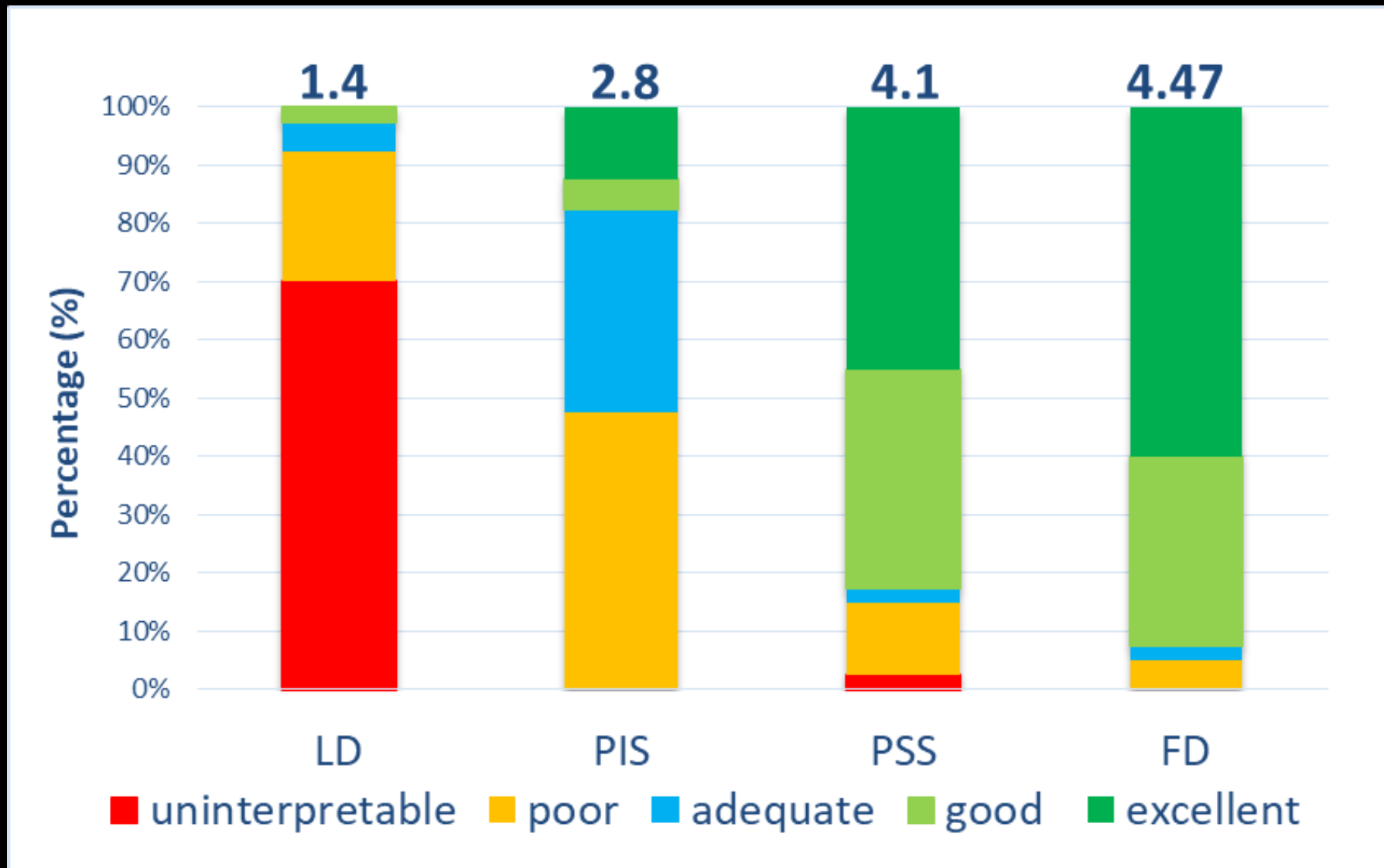
Deep learning for low-dose PET reconstruction



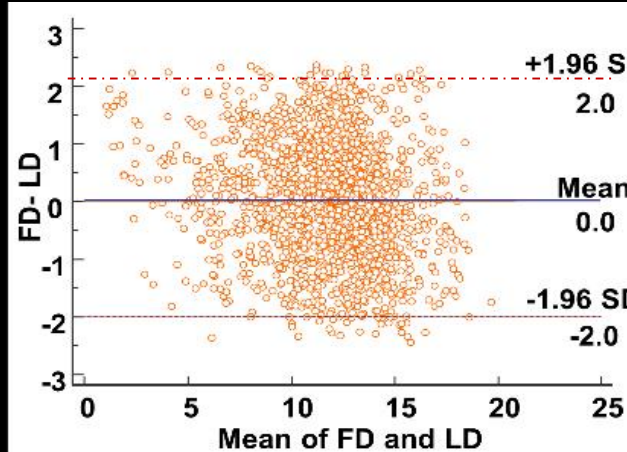
Deep learning for low-dose PET reconstruction



Deep learning for low-dose PET reconstruction



Bland-Altman analysis (Regionwise)



Low Dose

SUV_{mean} of 83 Regions

Based on “Hammersmith atlas”; n30r83

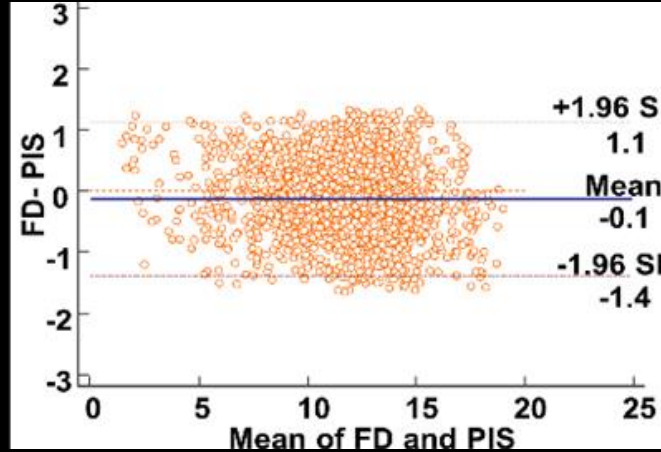
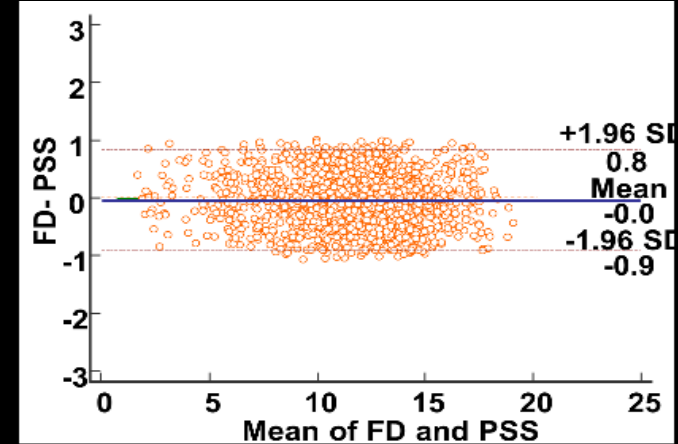
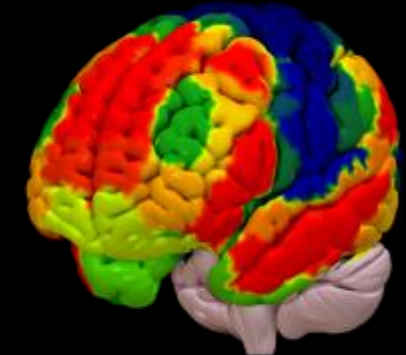


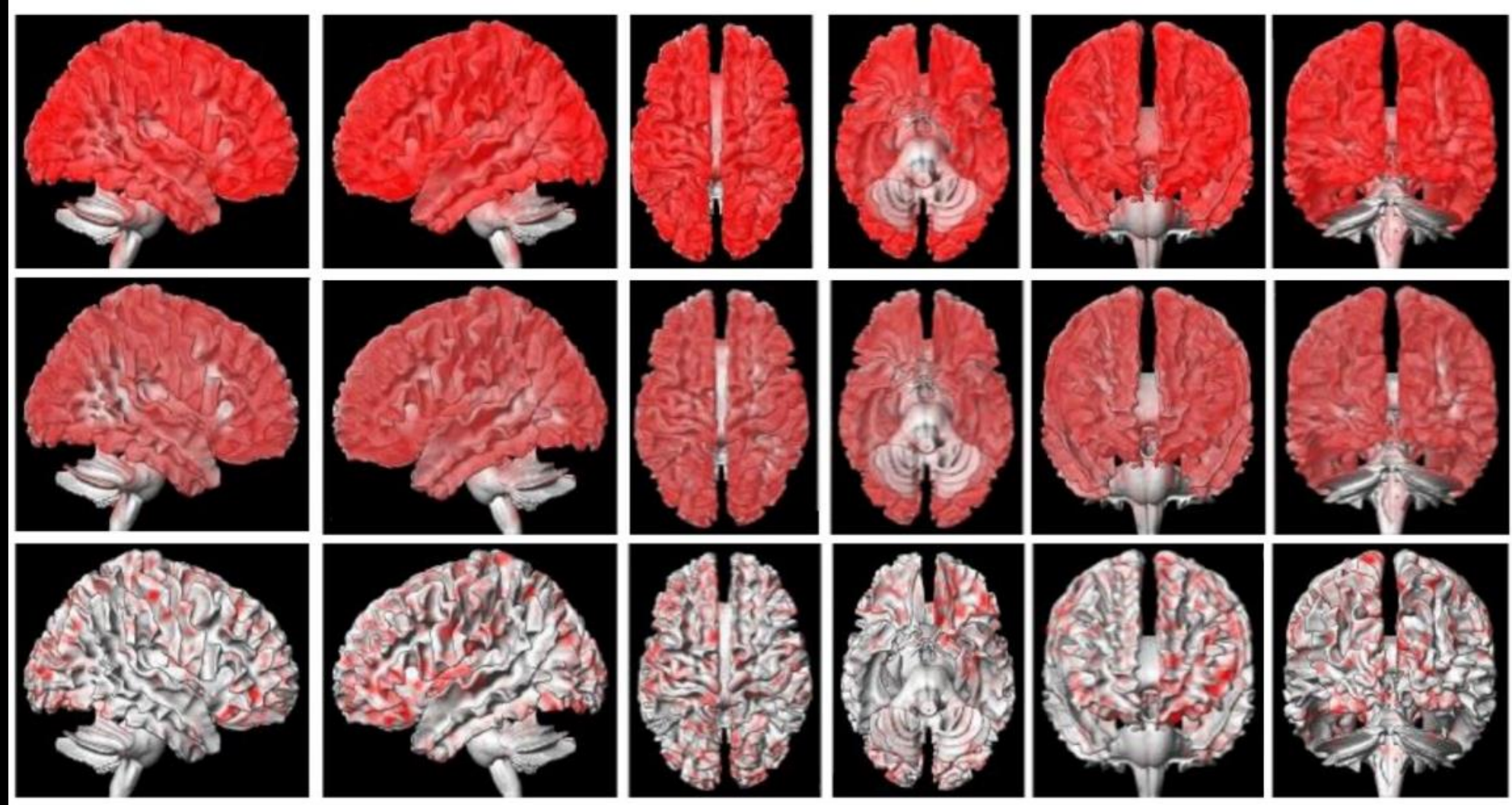
Image Space



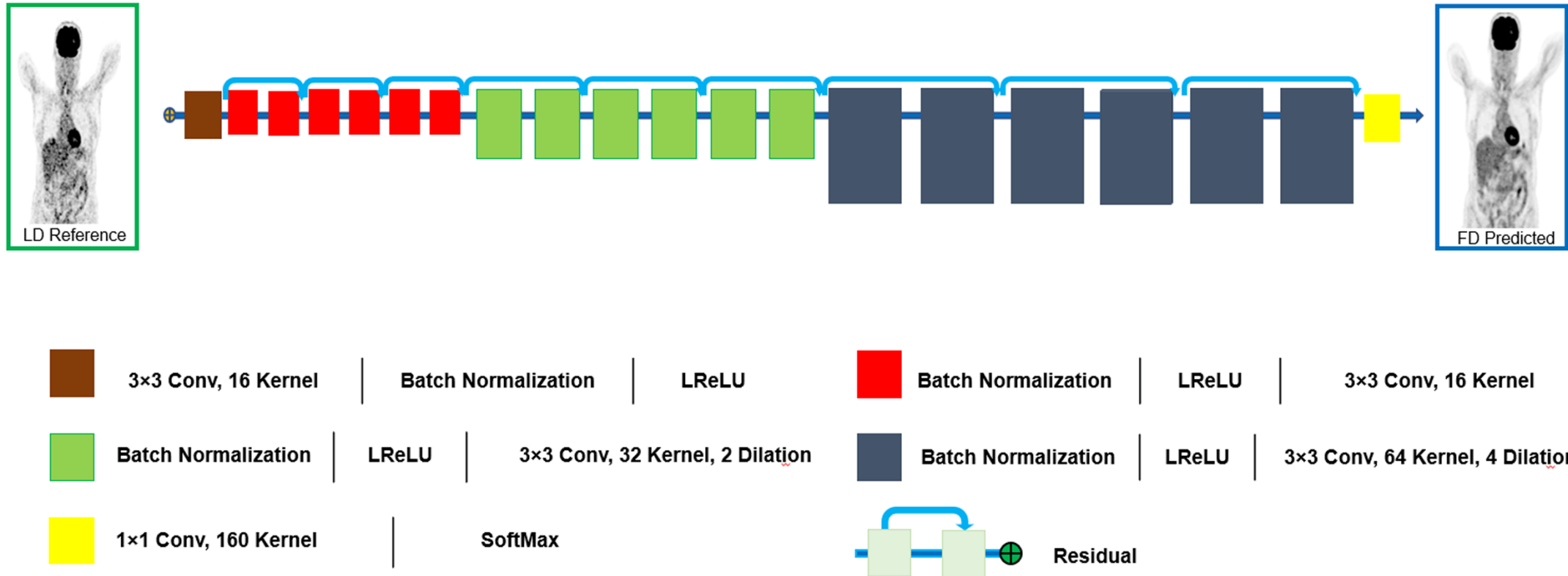
Sinogram Space



Deep learning for low-dose PET reconstruction



Deep learning-guided low-dose PET imaging



Deep learning-guided low-dose PET imaging

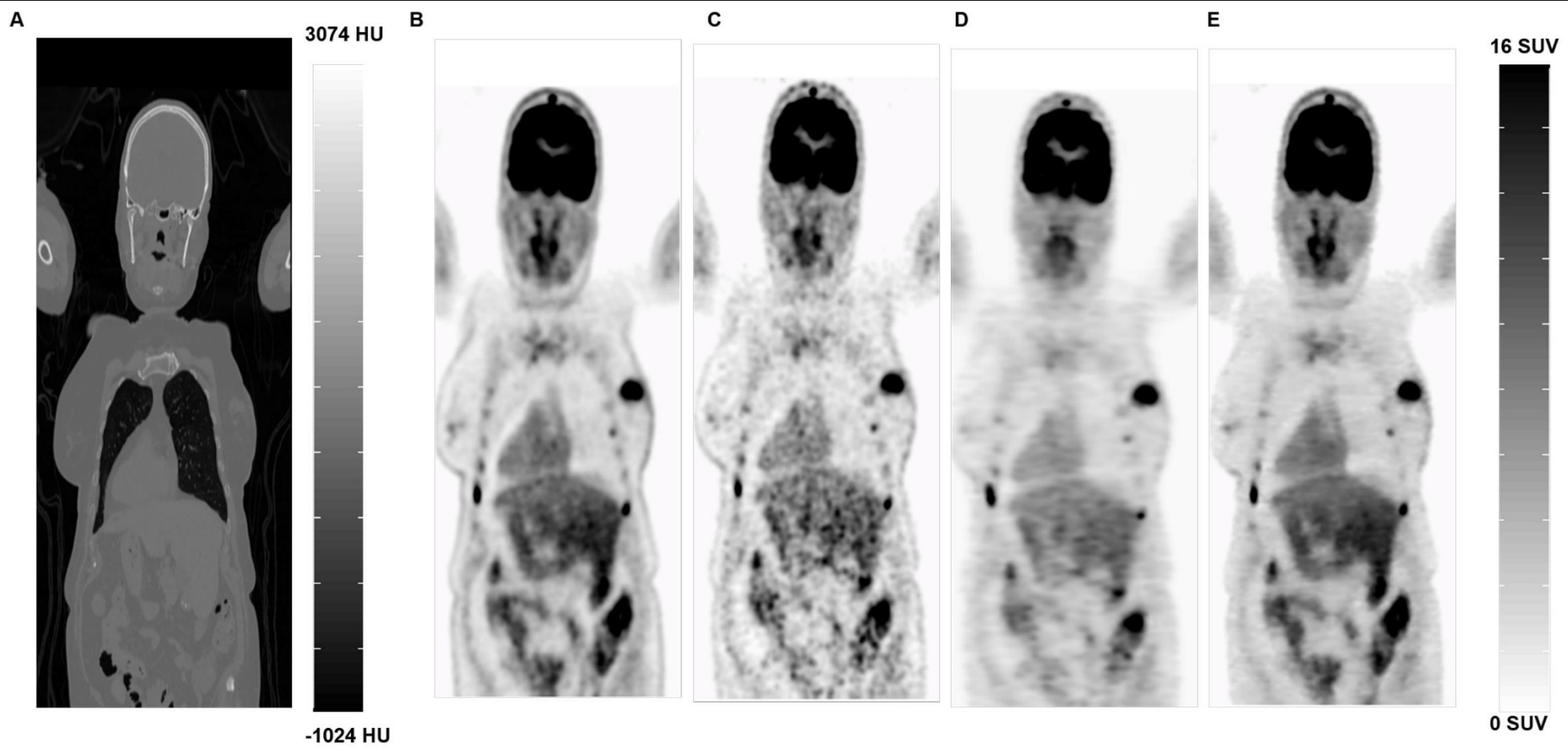
Low-dose CT

Full dose PET

Low dose PET

Pred. PET (RNET)

Pred. PET (CGAN)

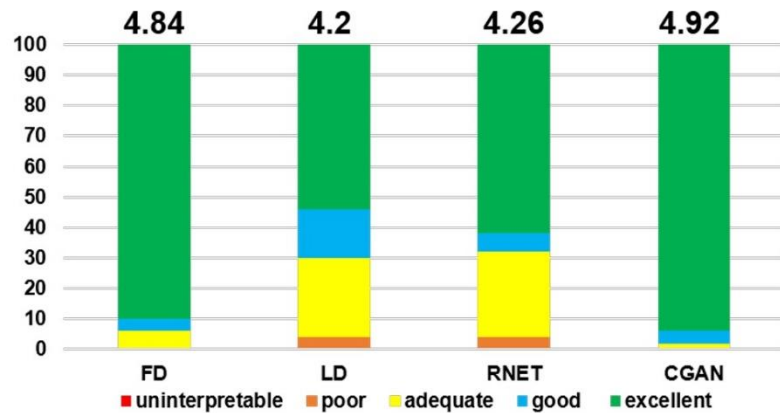


0.7 mm/s
(3 min/bed)

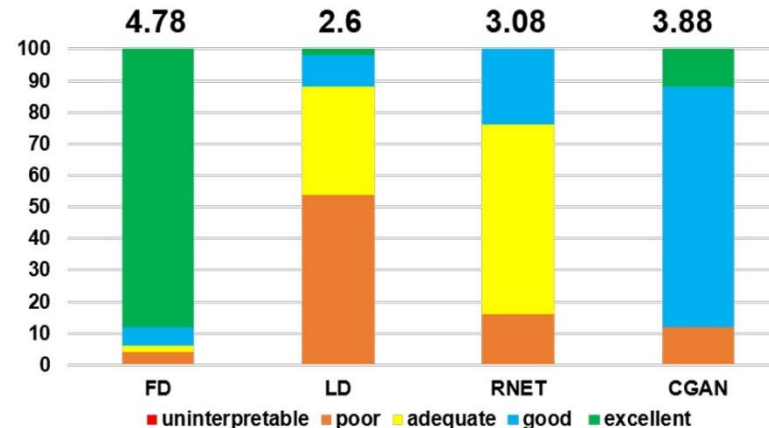
5 mm/s
(25 sec/bed)

Deep learning-guided low-dose PET imaging

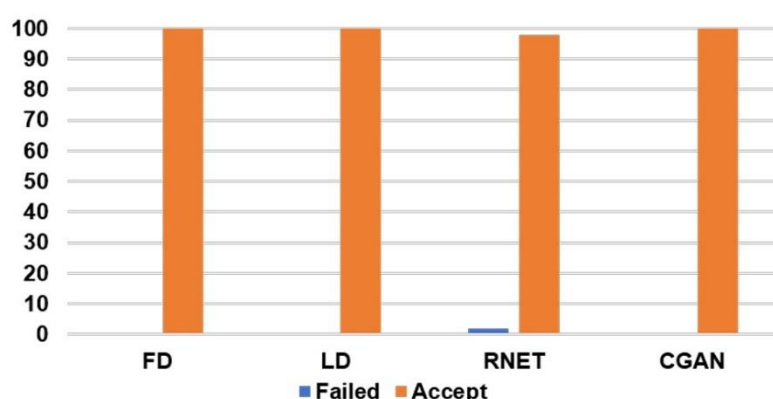
Zone 1 (Brain)



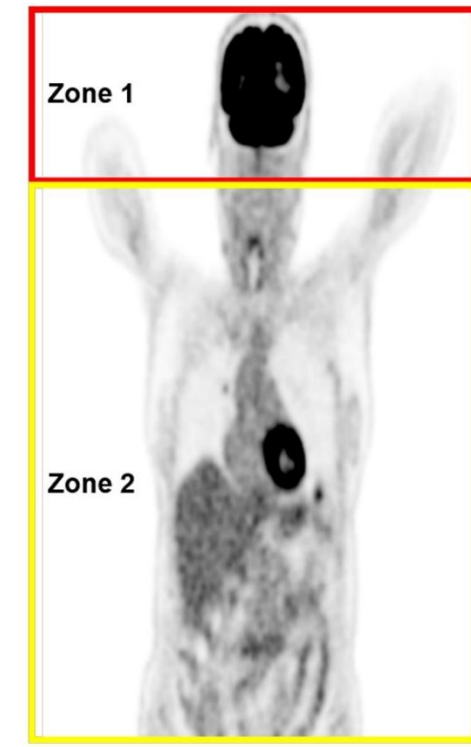
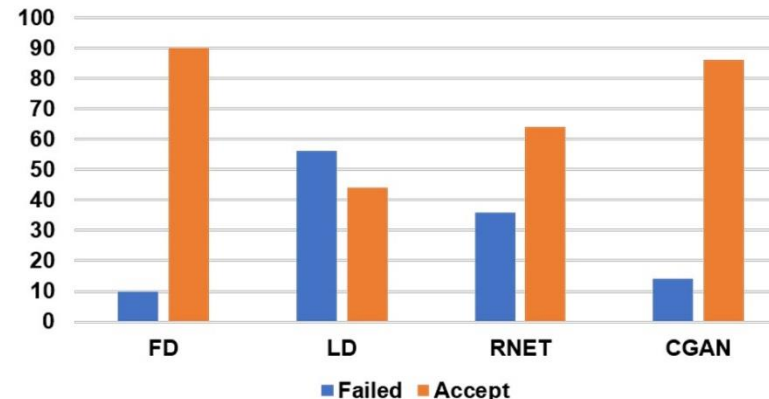
Zone 2 (Neck+Trunk)



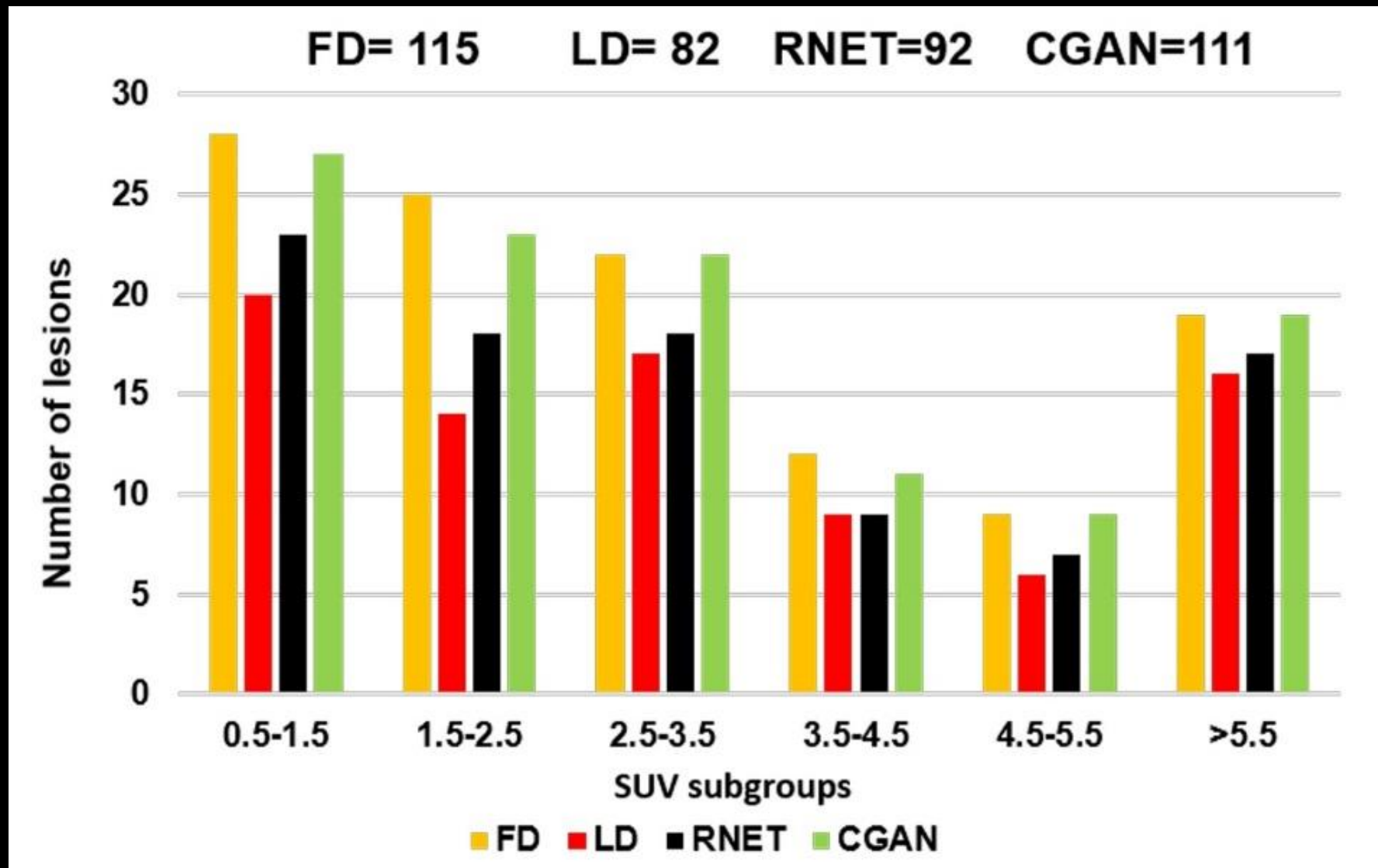
Zone 1 (Brain)



Zone 2 (Neck+Trunk)



Deep learning-guided low-dose PET imaging



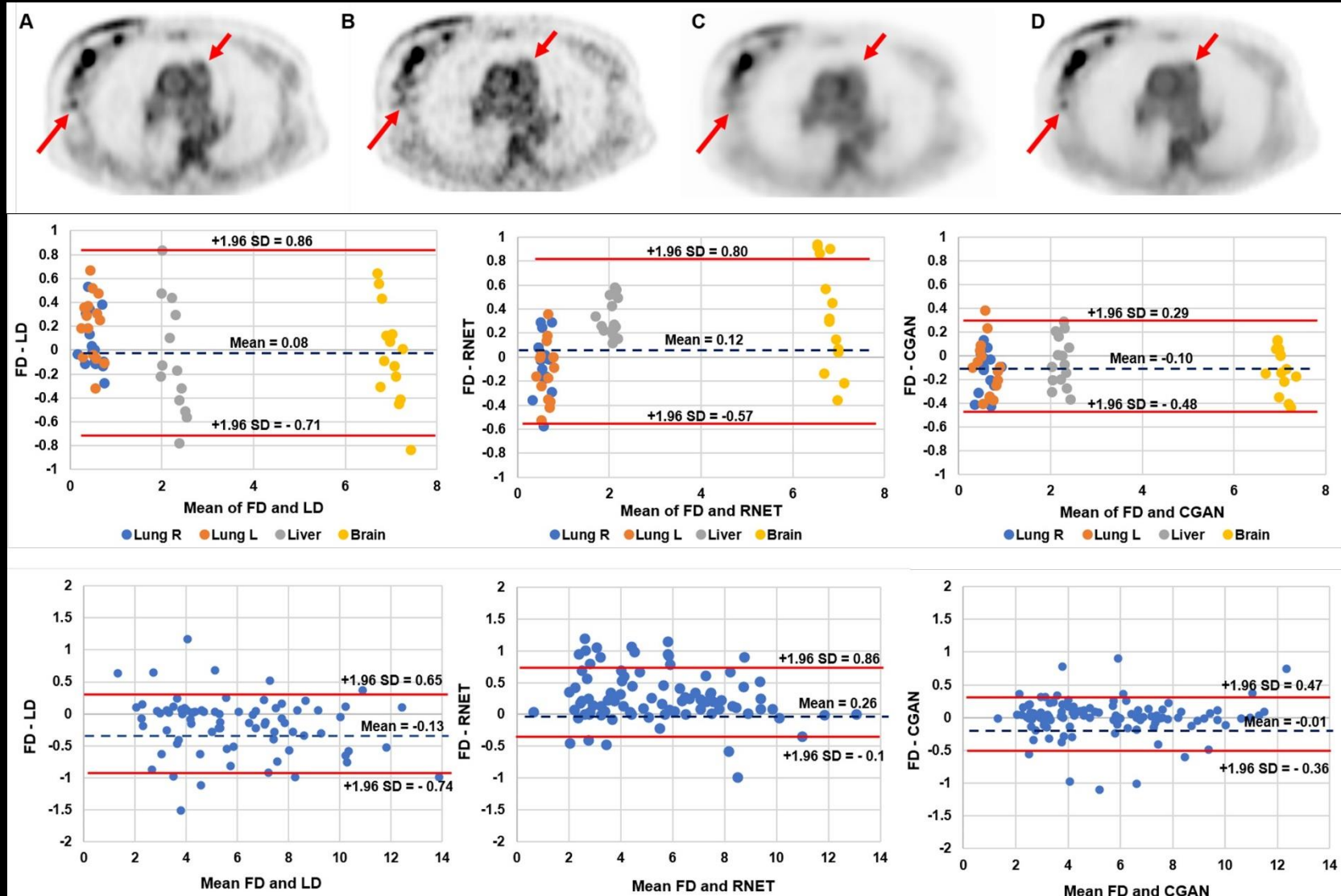
Deep learning-guided low-dose PET imaging

Full dose PET

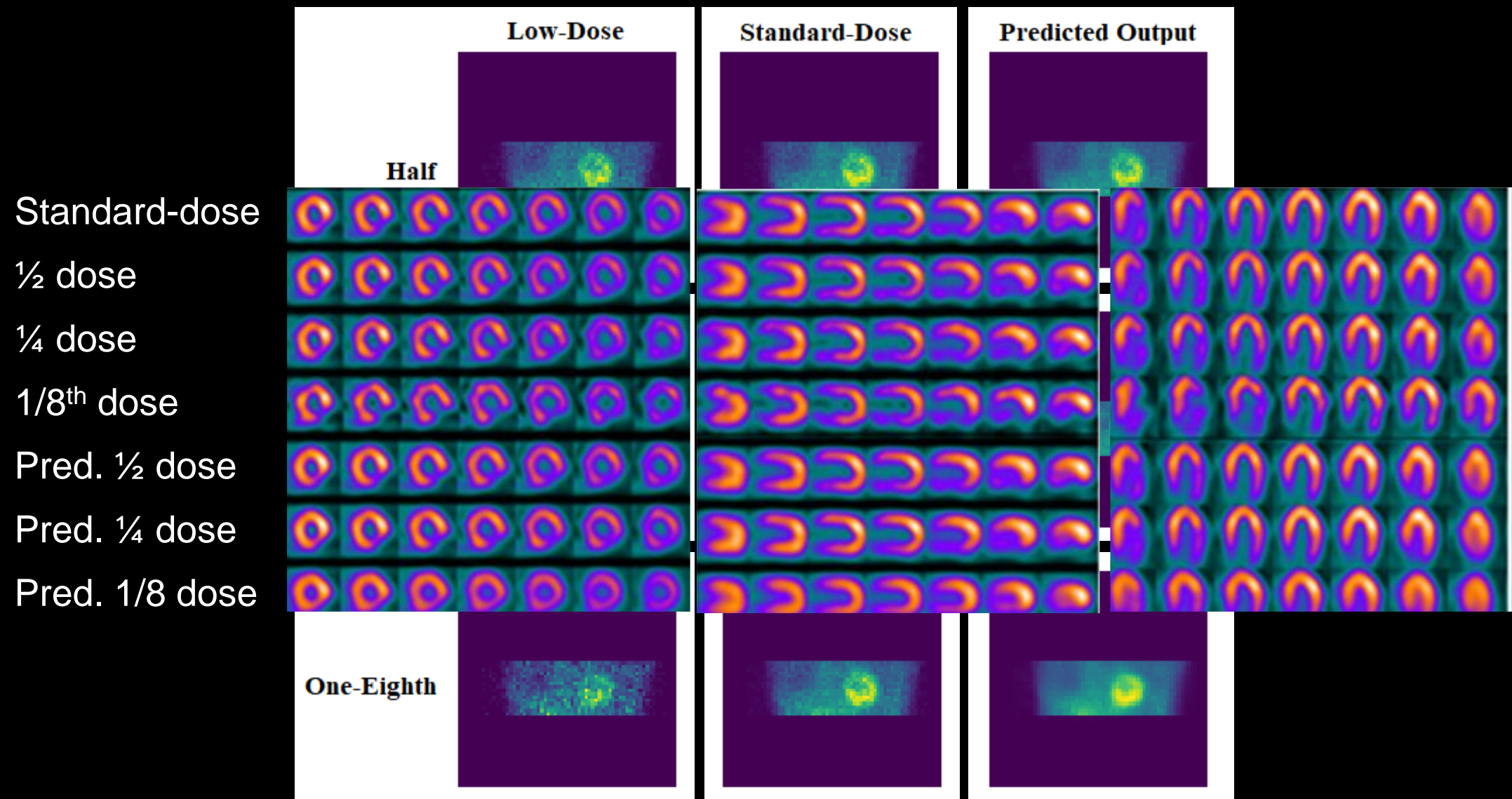
Low dose PET

Pred. PET (RNET)

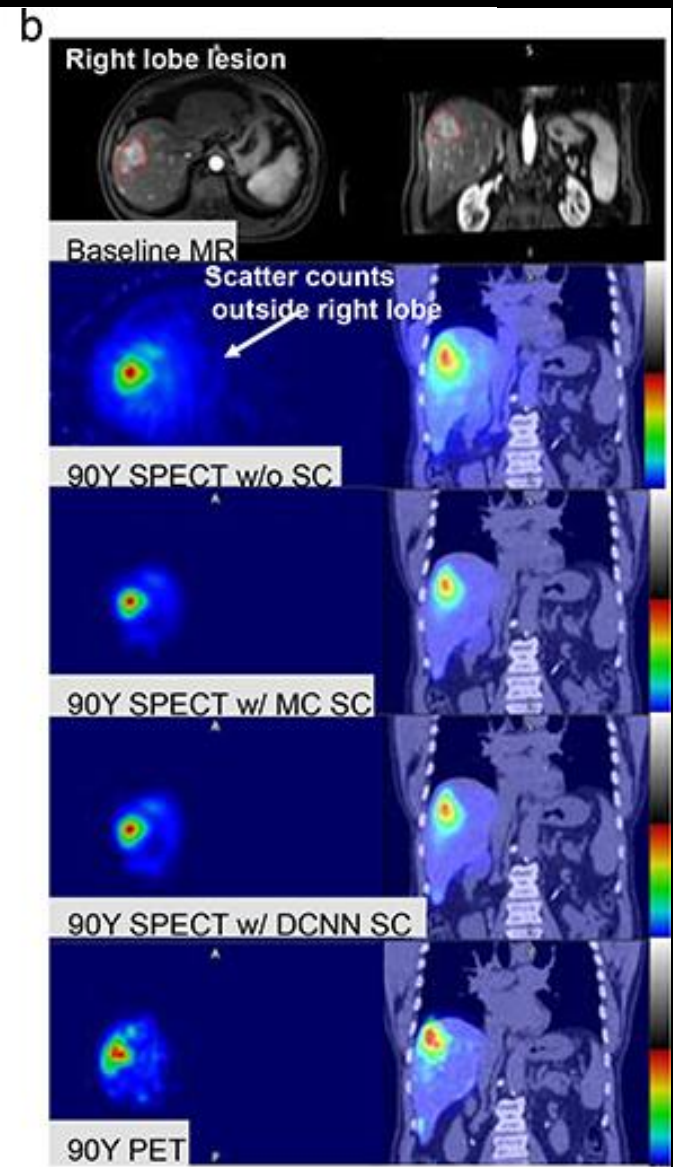
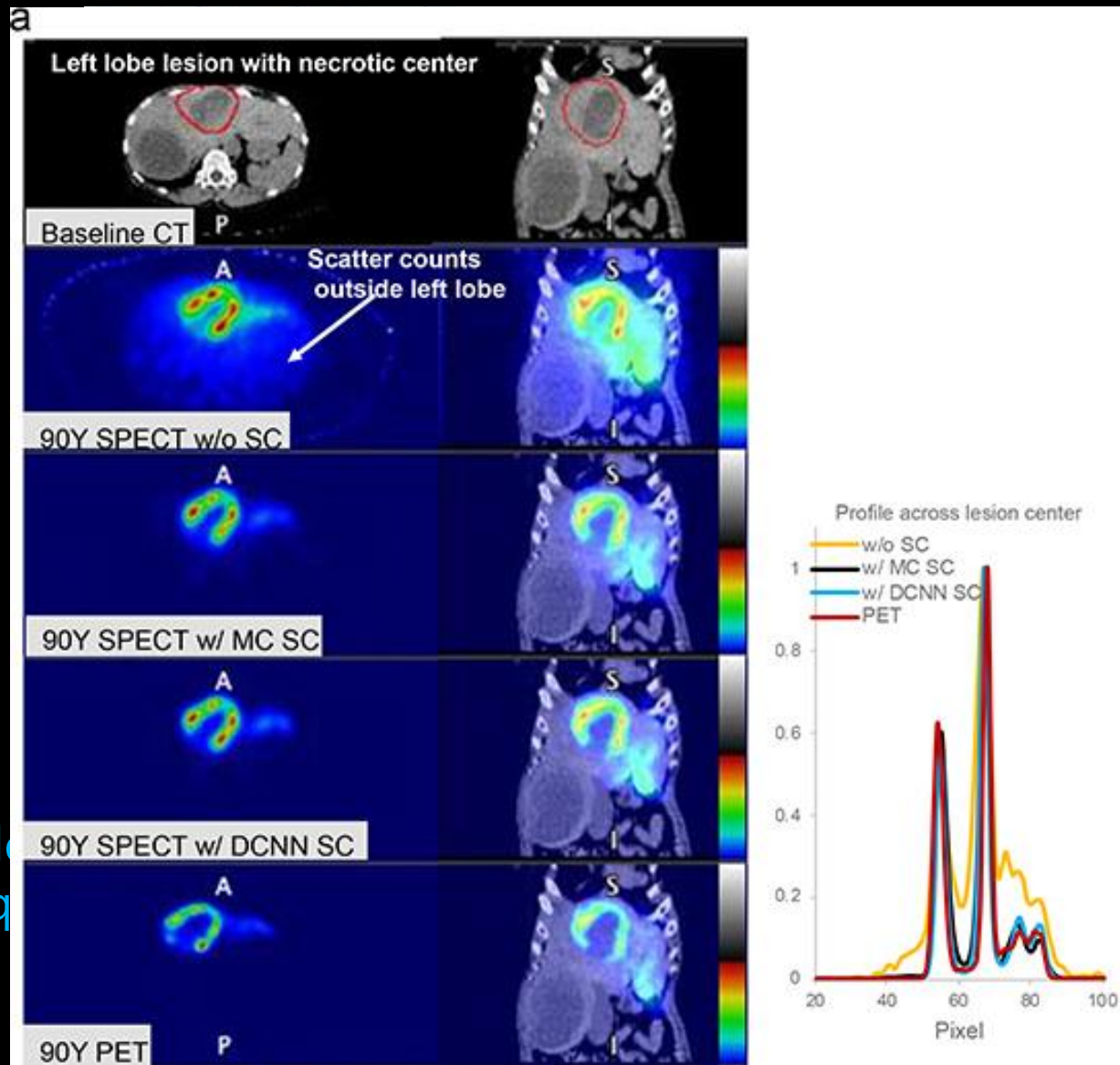
Pred. PET (CGAN)



Deep learning-guided low-dose MPI SPECT

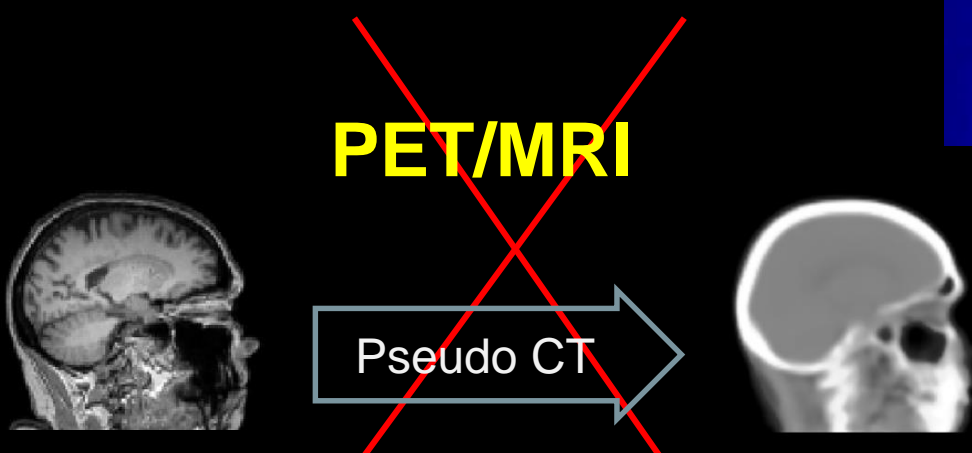
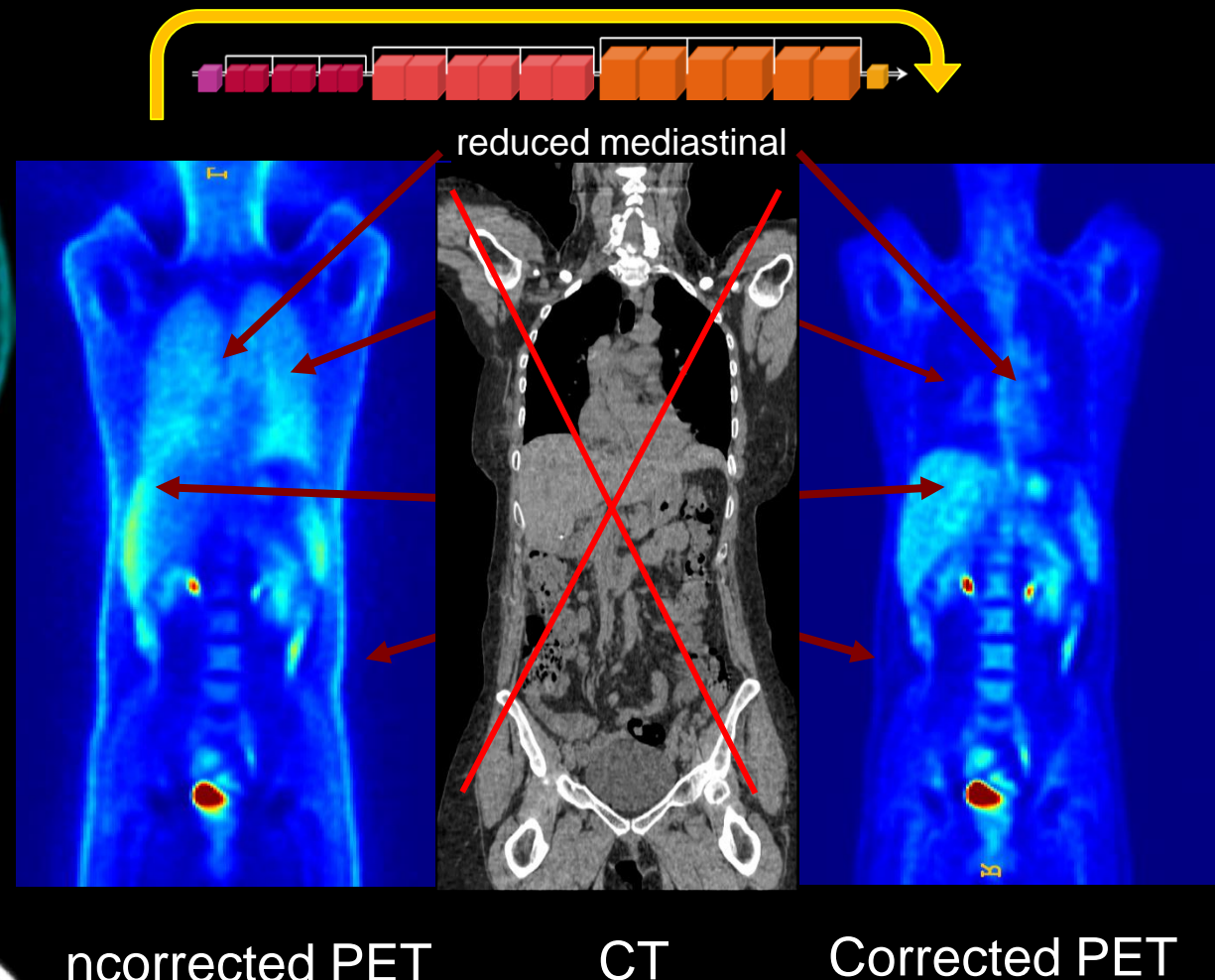
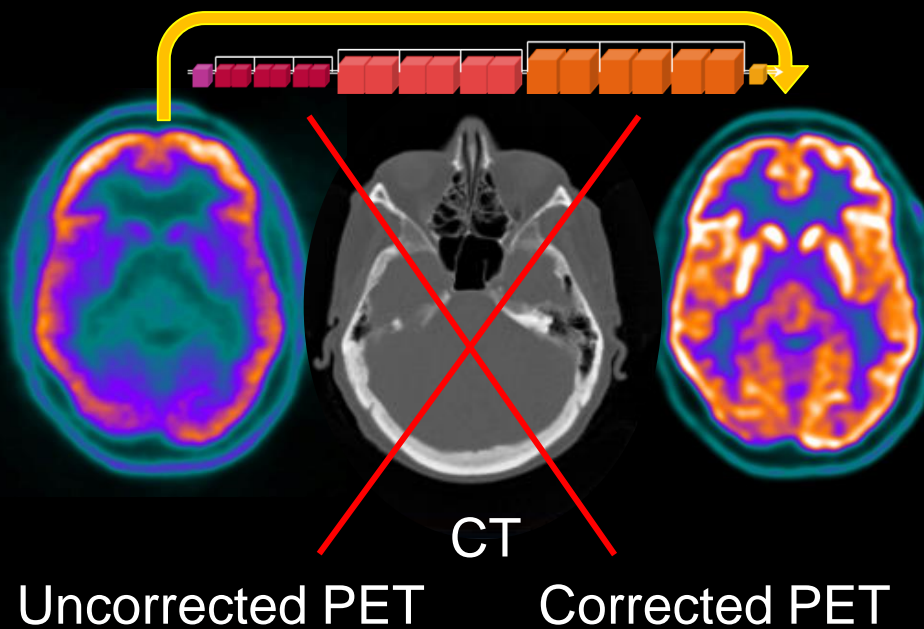


Deep learning-guided scatter correction

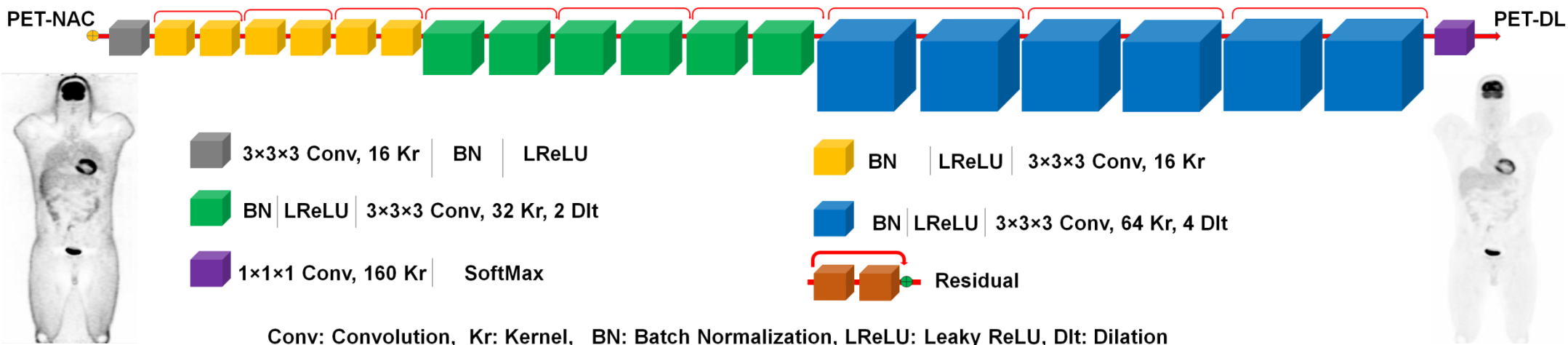


A
d
q

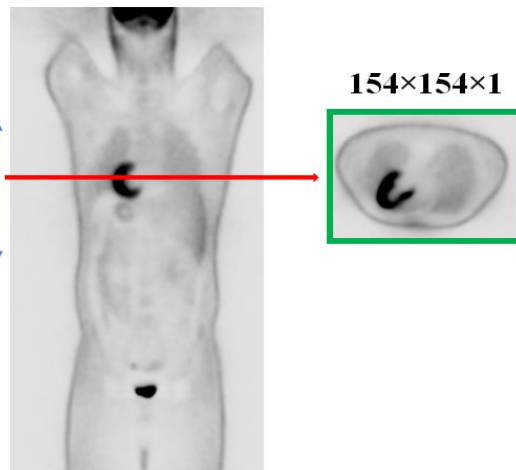
CT-based attenuation correction (Reference)



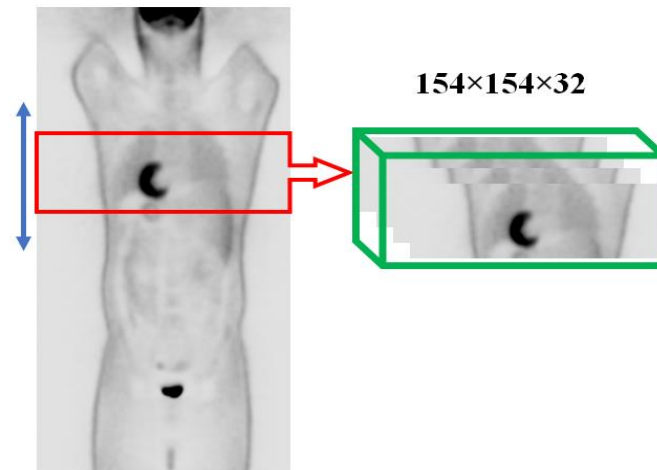
Deep learning-guided PET attenuation correction



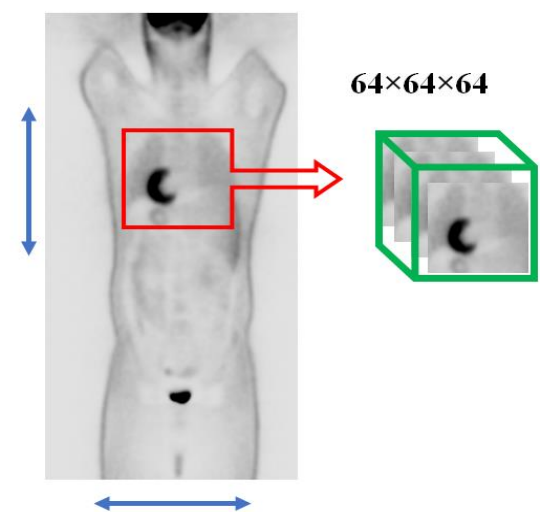
2D-Slc



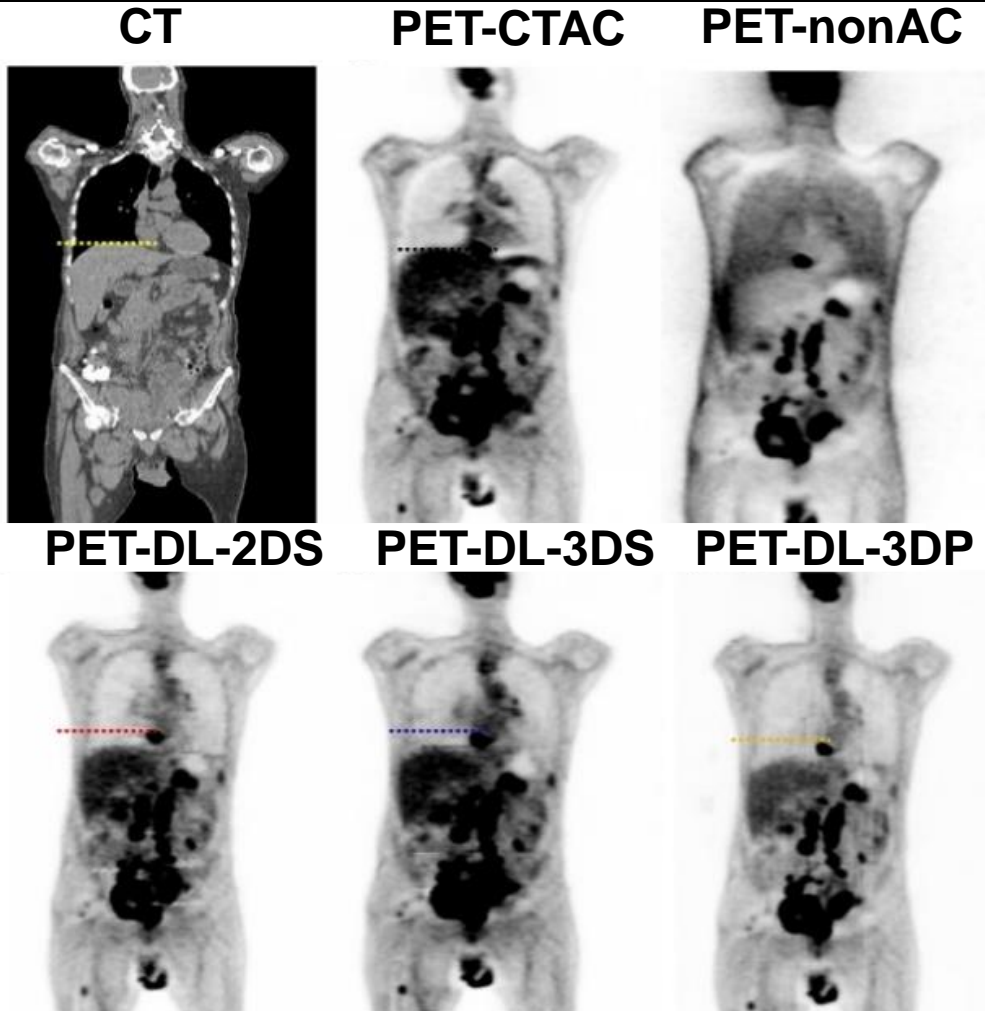
3D-Slc



3D-Pch

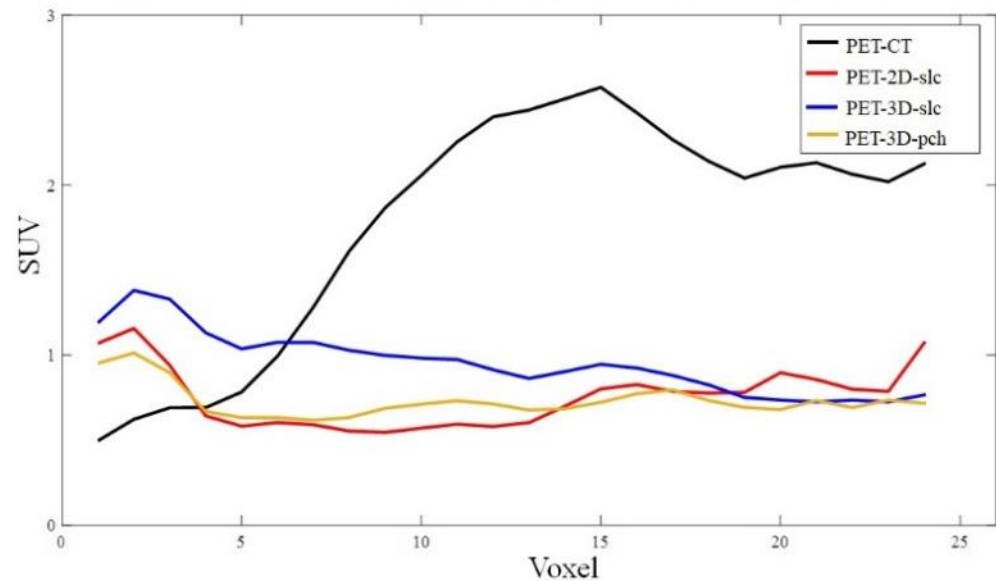
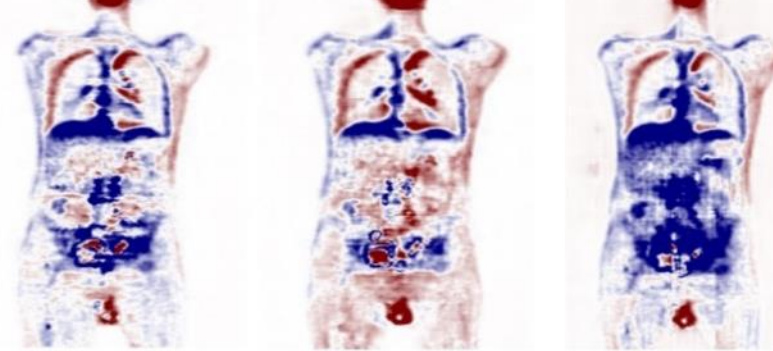


Deep learning compensates motion artifacts



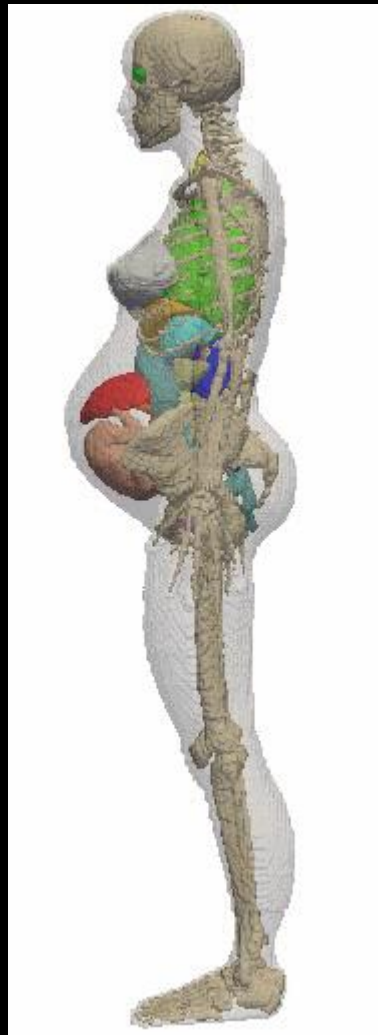
Difference images: PET-DL – PET-CTAC

PET-DL-2DS PET-DL-3DS PET-DL-3DP



Computational pregnant female phantoms

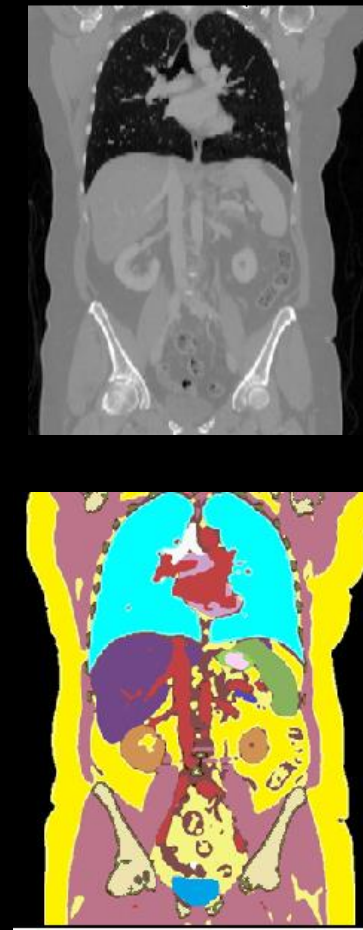
25w-gestation



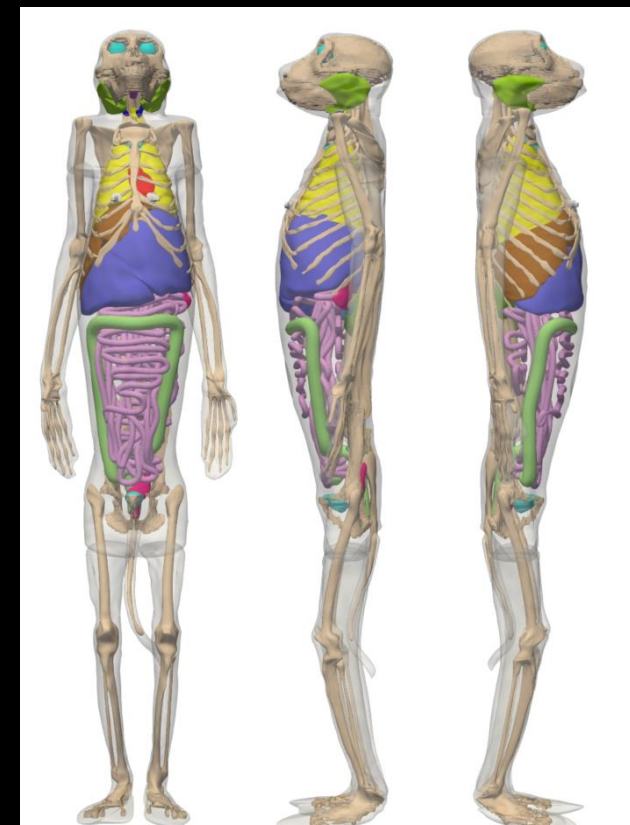
30w-gestation



Thorax-abdo

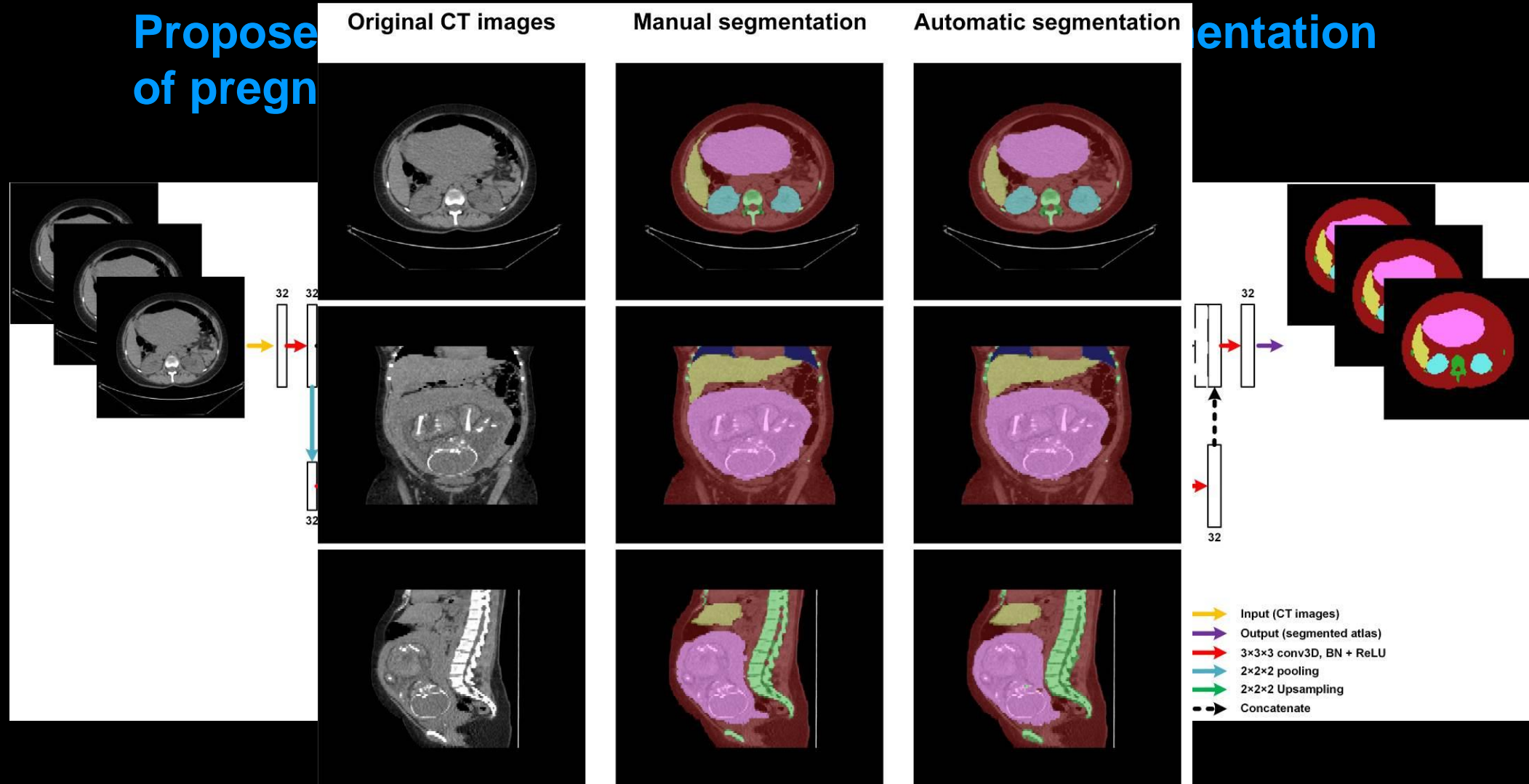


Non-human primate



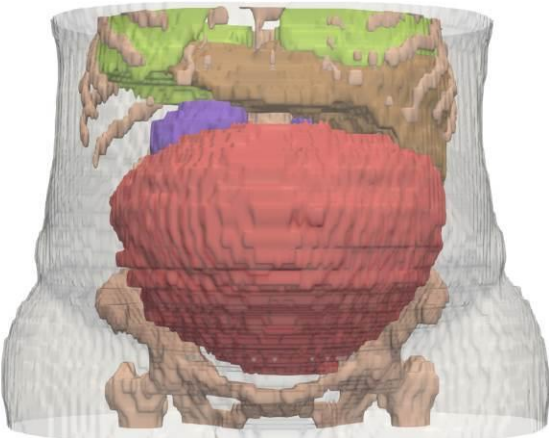
Automated generation of anatomical models

Propose
of pregn

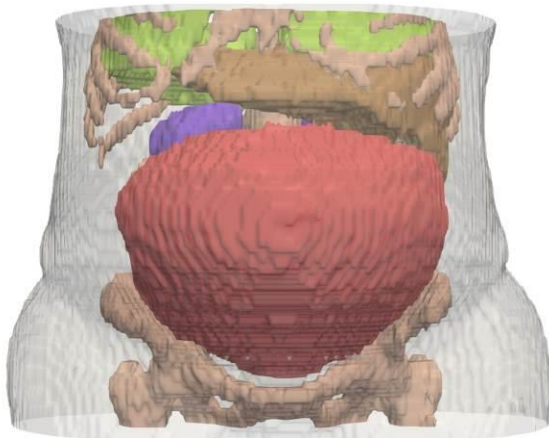


Automated generation of anatomical models

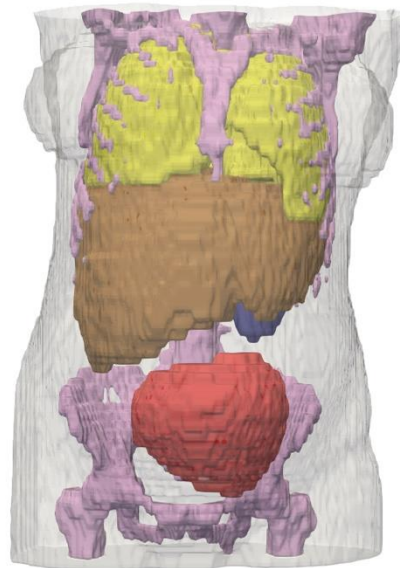
Manual segmentation



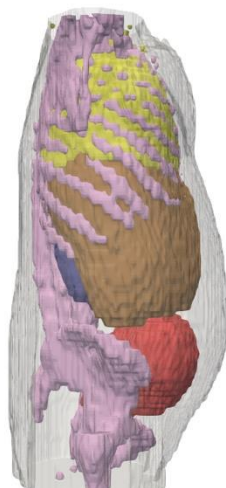
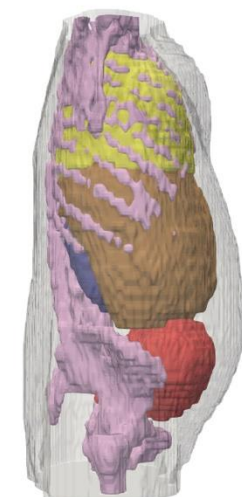
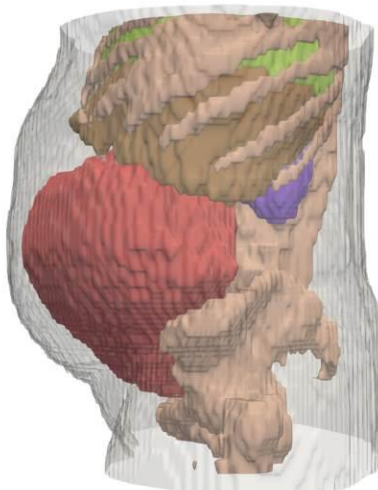
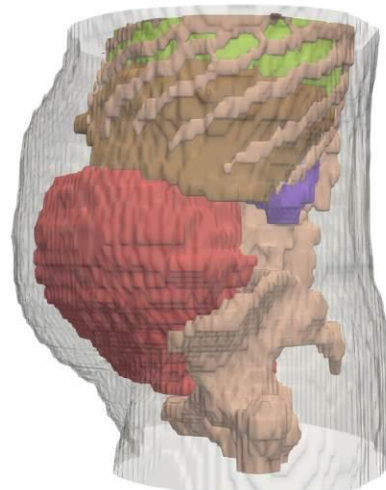
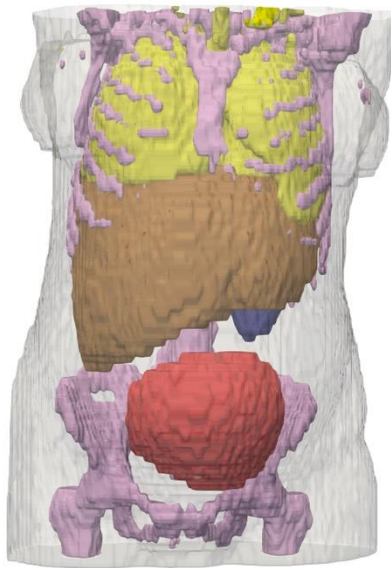
Automatic segmentation



Manual segmentation



Automatic segmentation



Deep learning in PET image segmentation

Medical Image Analysis 44 (2018) 177–195

Contents lists available at ScienceDirect

Medical Image Analysis

journal homepage: www.elsevier.com/locate/media



The first MICCAI challenge on PET tumor segmentation

Corrected: Author correction

Mathieu Hatt^{a,*}, Baptiste Laurent^a, Anouar Ouahabi^a, Hadi Fayad^a, Shan Tan^b, Laquan Li^b, Wei Lu^c, Vincent Jaouen^a, Clovis Tauber^d, Jakub Czakon^e, Filip Drapéjkowski^e, Witold Dyrka^{e,f}, Sorina Camarasu-Pop^g, Frédéric Cervenansky^g, Pascal Girard^g, Tristan Glatard^h, Michael Kainⁱ, Yao Yaoⁱ, Christian Barillotⁱ, Assen Kirov^c, Dimitris Visvikis^a

^aLaTIM, UMR 1101, INSERM, IBSAM, UBO, UBL, Brest, France

^bKey Laboratory of Image Processing and Intelligent Control of Ministry of Education of China, School of Automation, Huazhong University of Science and Technology, Wuhan 430074, China

^cMemorial Sloan-Kettering Cancer Center, New-York, USA

^dINSERM, UMR 930, Imaging and brain, University of Tours, France

^eStermedia Sp. z o. o., ul. A. Ostrowskiego 13, Wrocław, Poland

^fWroclaw University of Science and Technology, Faculty of Fundamental Problems of Technology, Department of Biomedical Engineering, Poland

^gUniversité de Lyon, CREATIS, CNRS UMR5220, INSERM UMR 1044, INSA-Lyon, Université Lyon 1, Lyon, France

^hDepartment of Computer Science and Software Engineering, Concordia University, Montreal, Canada

ⁱINRIA, Visages project-team, CNRS, IRISA 6074, INSERM, Visages, UMR 1228, University of Rennes 1, Rennes Cx 35042, France

ARTICLE INFO

Article history:

Received 5 May 2017

Revised 7 December 2017

Accepted 7 December 2017

Available online 9 December 2017

Keywords:

PET functional volumes

Image segmentation

MICCAI challenge

Comparative study

ABSTRACT

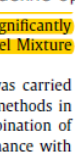
Introduction: Automatic functional volume segmentation in PET images is a challenge that has been addressed using a large array of methods. A major limitation for the field has been the lack of dataset that would allow direct comparison of the results in the various publications. In the work we describe a comparison of recent methods on a large dataset following recommendations of the American Association of Physicists in Medicine (AAPM) task group (TG) 211, which was carried out in the framework of the first MICCAI (Medical Image Computing and Computer Assisted Intervention) challenge.

Materials and methods: Organization and funding was provided by France Life Imaging (FLI) of 176 images combining simulated, phantom and clinical images was assembled. A website was created for participants to register and download training data ($n=19$). Challengers then submitted their pipelines on an online platform that autonomously ran the algorithms on the testing data and evaluated the results. The methods were ranked according to the arithmetic mean of sensitivity and predictive value.

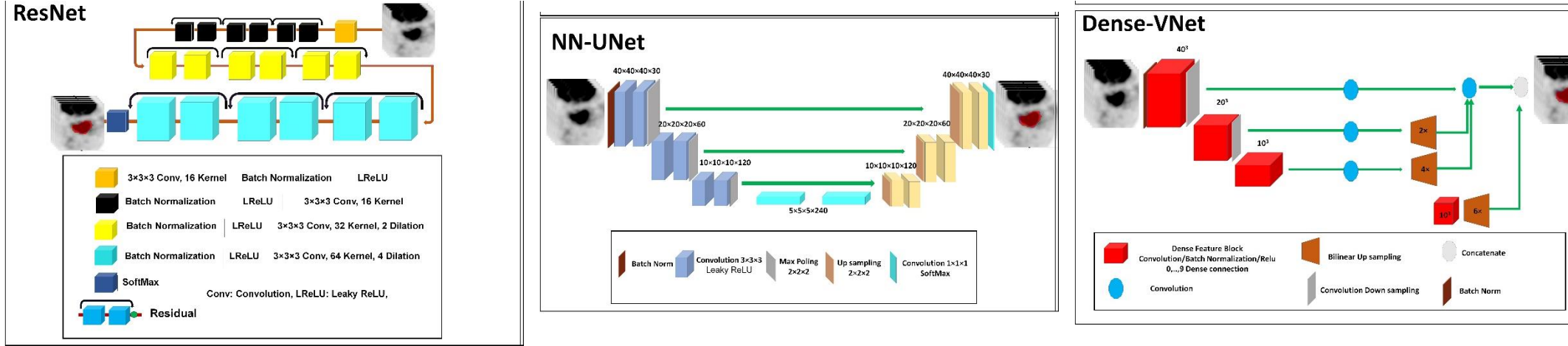
Results: Sixteen teams registered but only four provided manuscripts and pipeline(s) for review. In addition, results using two thresholds and the Fuzzy Locally Adaptive Bayesian generated. All competing methods except one performed with median accuracy above 0.8. The method with the highest score was the convolutional neural network-based segmentation, which significantly outperformed 9 out of 12 of the other methods, but not the improved K-Means, Gaussian Model Mixture and Fuzzy C-Means methods.

Conclusion: The most rigorous comparative study of PET segmentation algorithms to date was carried out using a dataset that is the largest used in such studies so far. The hierarchy amongst the methods in terms of accuracy did not depend strongly on the subset of datasets or the metrics (or combination of metrics). All the methods submitted by the challengers except one demonstrated good performance with median accuracy scores above 0.8.

International challenges have become the standard for validation of biomedical image analysis methods. Given their scientific impact, it is surprising that a critical analysis of common practices related to the organization of challenges has not yet been performed. In this paper, we present a comprehensive analysis of biomedical image analysis challenges conducted up to now. We demonstrate the importance of challenges and show that the lack of quality control has critical consequences. First, reproducibility and interpretation of the results is often hampered as only a fraction of relevant information is typically provided. Second, the rank of an algorithm is generally not robust to a number of variables such as the test data used for validation, the ranking scheme applied and the observers that make the reference annotations. To overcome these problems, we recommend best practice guidelines and define open research questions to be addressed in the future.

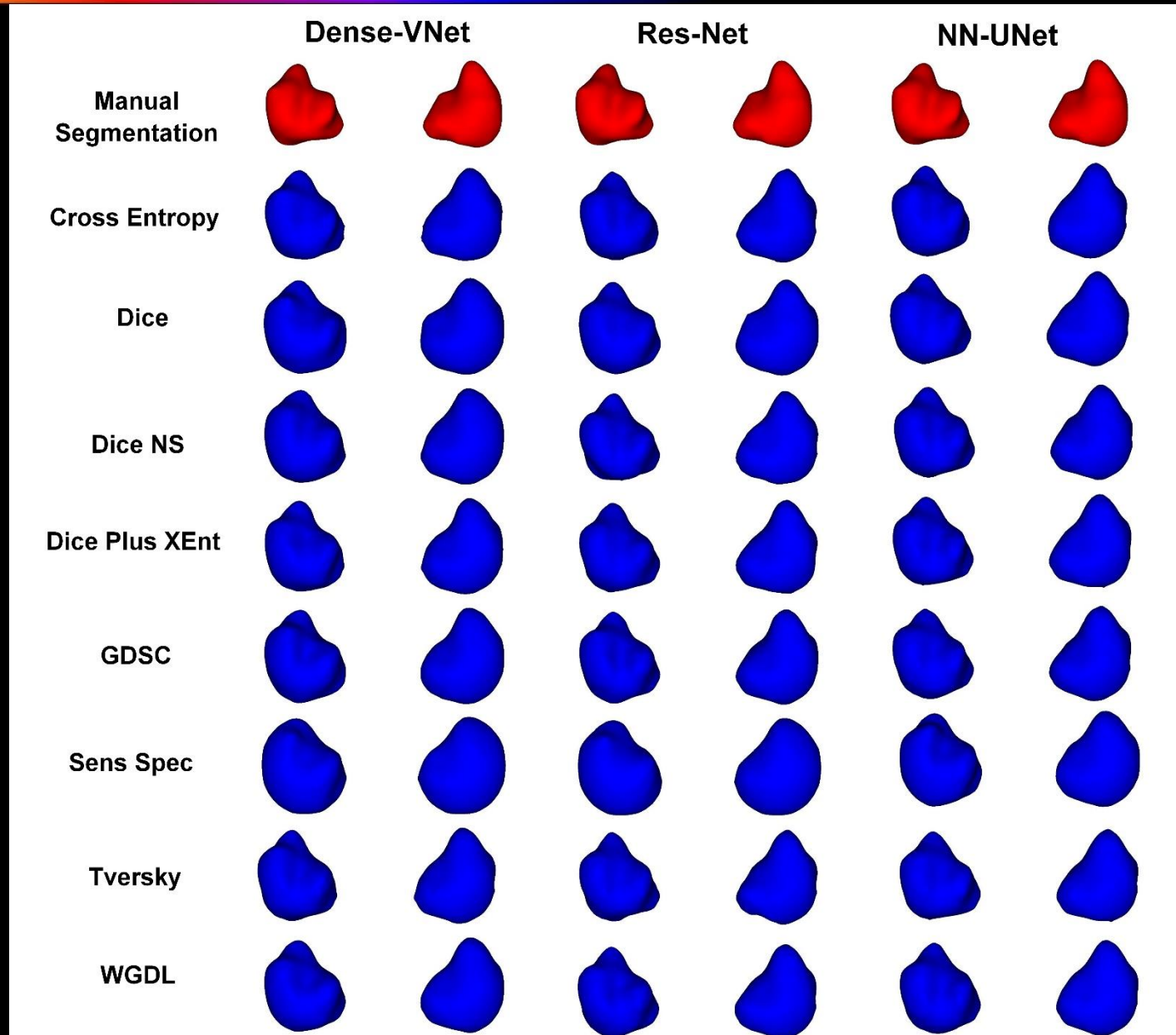


Deep learning-guided PET segmentation



- Evaluate 3 state-of-the-art deep learning algorithms (ResNET, NN-Unet, Dense-Vnet) combined with 8 different loss functions (Dice, generalized Wasserstein Dice loss, Dice Plus Xent loss, generalized Dice loss, cross-entropy, sensitivity-specificity, and Tversky) for PET image segmentation using a comprehensive training set (340) and evaluated its performance on an external validation set (100) of head and neck cancer patients.

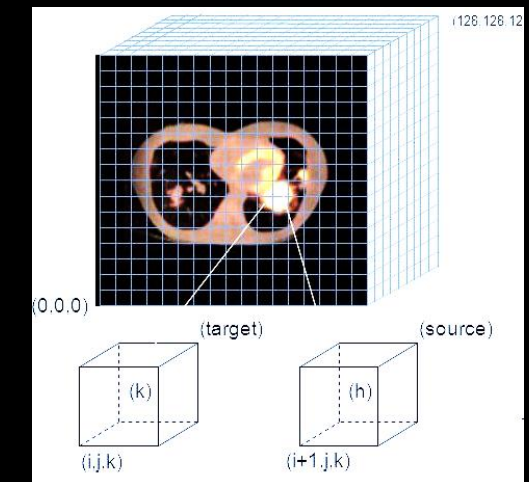
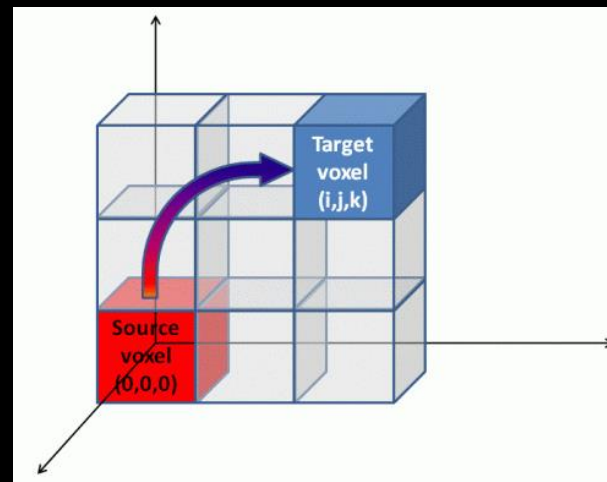
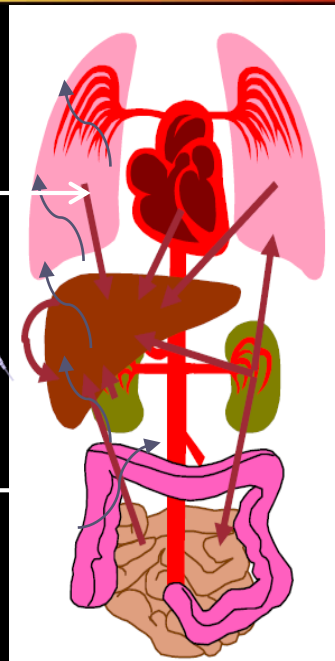
Deep learning-guided PET segmentation



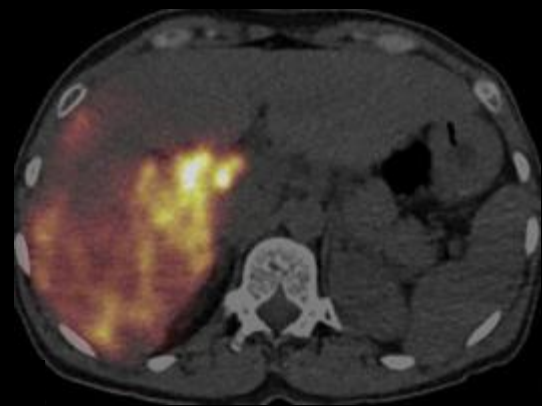
Deep learning-guided PET segmentation

Method	Loss Function	Dice	Jaccard	False Negative	False Positive	Volume Similarity	Mean Surface Distance	Std Surface Distance	Max Surface Distance
Dense-VNET	Cross Entropy	0.82 - 0.85	0.71 - 0.74	0.10 - 0.14	0.16 - 0.20	0.03 - 0.11	0.17 - 0.2	0.40 - 0.45	2.1 - 2.4
	Dice	0.75 - 0.78	0.61 - 0.65	0.05 - 0.09	0.30 - 0.34	0.26 - 0.35	0.26 - 0.30	0.51 - 0.56	2.6 - 3.0
	Dice NS	0.76 - 0.79	0.62 - 0.66	0.04 - 0.08	0.29 - 0.33	0.27 - 0.36	0.25 - 0.28	0.48 - 0.52	2.4 - 2.7
	Dice Plus XEnt	0.80 - 0.82	0.67 - 0.71	0.05 - 0.08	0.24 - 0.28	0.19 - 0.27	0.20 - 0.23	0.43 - 0.48	2.2 - 2.5
	GDSC	0.75 - 0.78	0.61 - 0.65	0.05 - 0.09	0.30 - 0.34	0.27 - 0.36	0.27 - 0.30	0.51 - 0.56	2.7 - 3.0
	Sens Spec	0.70 - 0.72	0.54 - 0.57	0.03 - 0.06	0.40 - 0.44	0.45 - 0.53	0.35 - 0.38	0.61 - 0.65	2.9 - 3.2
	Tversky	0.82 - 0.85	0.71 - 0.74	0.11 - 0.15	0.16 - 0.19	0.01 - 0.09	0.17 - 0.20	0.40 - 0.45	2.0 - 2.3
	WGDL	0.74 - 0.76	0.59 - 0.63	0.04 - 0.07	0.34 - 0.38	0.34 - 0.42	0.29 - 0.32	0.53 - 0.57	2.6 - 2.9
Res-Net	Cross Entropy	0.84 - 0.86	0.73 - 0.76	0.1 - 0.14	0.14 - 0.17	0.00 - 0.07	0.16 - 0.19	0.38 - 0.43	1.9 - 2.3
	Dice	0.83 - 0.85	0.71 - 0.74	0.06 - 0.09	0.20 - 0.23	0.13 - 0.20	0.17 - 0.20	0.39 - 0.43	2.0 - 2.3
	Dice NS	0.83 - 0.85	0.71 - 0.75	0.07 - 0.11	0.18 - 0.22	0.08 - 0.16	0.17 - 0.20	0.40 - 0.45	2.1 - 2.4
	Dice Plus XEnt	0.83 - 0.85	0.72 - 0.75	0.07 - 0.11	0.18 - 0.21	0.07 - 0.15	0.16 - 0.19	0.39 - 0.43	2.0 - 2.3
	GDSC	0.82 - 0.84	0.71 - 0.74	0.06 - 0.09	0.20 - 0.24	0.13 - 0.20	0.17 - 0.20	0.40 - 0.45	2.1 - 2.4
	Sens Spec	0.71 - 0.73	0.55 - 0.58	0.03 - 0.06	0.38 - 0.42	0.41 - 0.50	0.33 - 0.37	0.59 - 0.63	2.8 - 3.1
	Tversky	0.83 - 0.86	0.72 - 0.75	0.099 - 0.14	0.15 - 0.18	0.02 - 0.09	0.16 - 0.19	0.38 - 0.43	2.0 - 2.3
	WGDL	0.83 - 0.85	0.72 - 0.75	0.061 - 0.09	0.19 - 0.23	0.12 - 0.19	0.16 - 0.19	0.38 - 0.43	1.9 - 2.3
NN-UNet	Cross Entropy	0.81 - 0.83	0.69 - 0.72	0.06 - 0.1	0.21 - 0.25	0.13 - 0.21	0.19 - 0.22	0.43 - 0.5	2.2 - 2.7
	Dice	0.82 - 0.85	0.71 - 0.74	0.06 - 0.09	0.20 - 0.24	0.13 - 0.20	0.18 - 0.21	0.41 - 0.46	2.1 - 2.4
	Dice NS	0.82 - 0.85	0.71 - 0.74	0.05 - 0.08	0.21 - 0.24	0.15 - 0.22	0.17 - 0.21	0.40 - 0.45	2.0 - 2.3
	Dice Plus XEnt	0.84 - 0.86	0.73 - 0.76	0.08 - 0.12	0.16 - 0.19	0.05 - 0.12	0.16 - 0.19	0.39 - 0.46	2.0 - 2.5
	GDSC	0.82 - 0.85	0.71 - 0.74	0.06 - 0.1	0.19 - 0.23	0.11 - 0.19	0.17 - 0.21	0.40 - 0.46	2.0 - 2.4
	Sens Spec	0.71 - 0.74	0.56 - 0.59	0.04 - 0.07	0.37 - 0.41	0.39 - 0.48	0.32 - 0.36	0.58 - 0.62	2.9 - 3.2
	Tversky	0.80 - 0.83	0.68 - 0.72	0.09 - 0.13	0.20 - 0.23	0.08 - 0.17	0.20 - 0.24	0.45 - 0.52	2.3 - 2.8
	WGDL	0.82 - 0.85	0.71 - 0.74	0.05 - 0.08	0.20 - 0.24	0.15 - 0.22	0.17 - 0.20	0.40 - 0.45	2.0 - 2.4

Voxel-based internal dosimetry (MIRD)

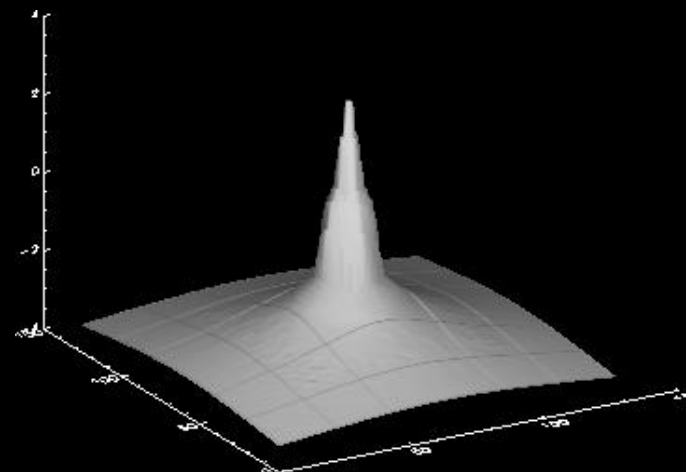


$$\bar{D}_{voxel_k} = \sum_{n=1}^N \tilde{A}_{voxel_n} \cdot S(voxel_k \leftarrow voxel_n)$$



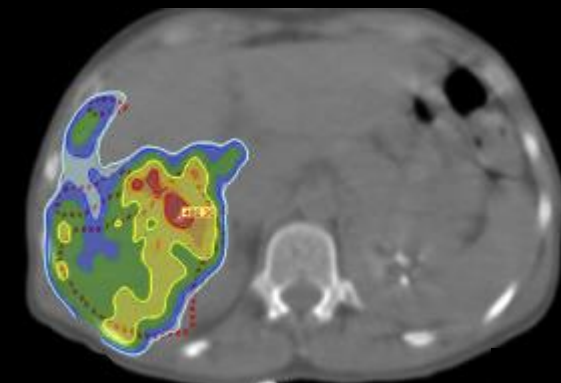
Activity map

*



Dose point kernel

=



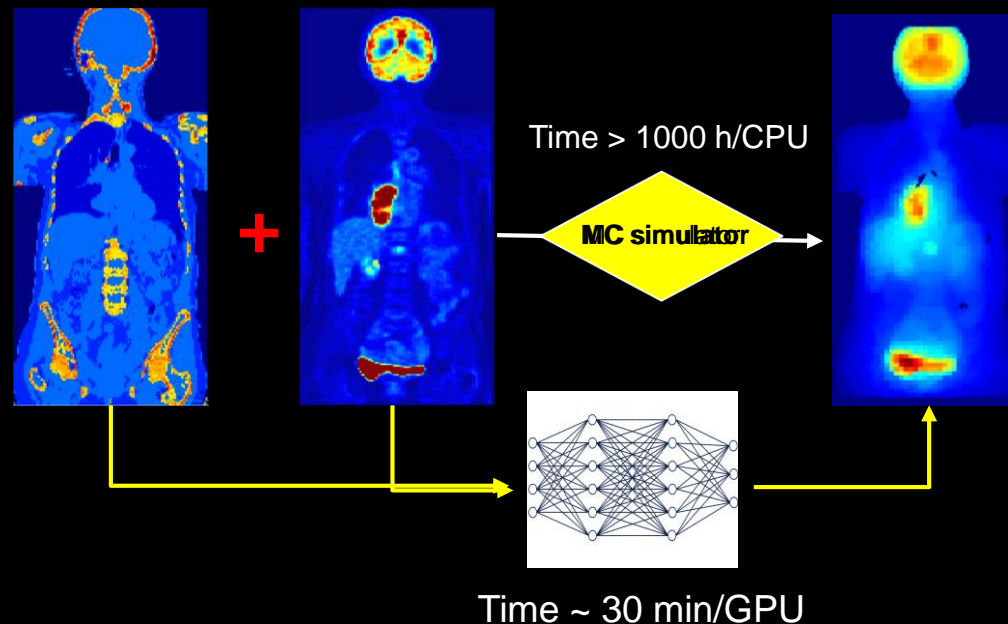
3D dose map

Monte Carlo → Reference (gold Standard)

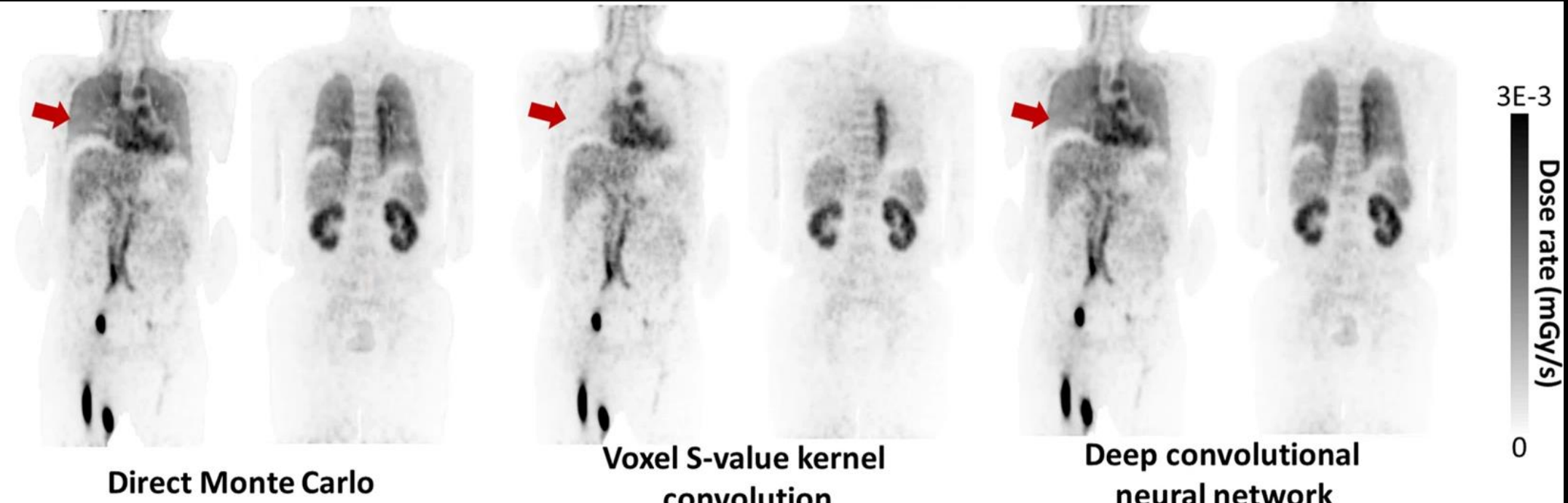
But heavy computational burden!!!



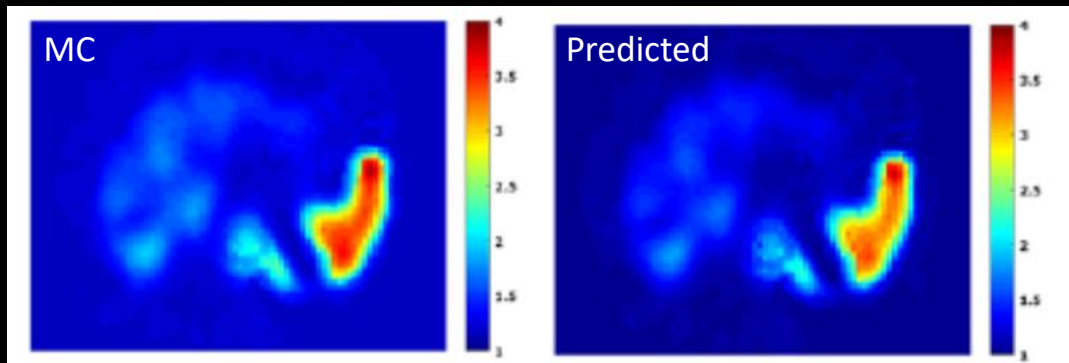
Monte Carlo-based dose mapping could be formulated as a regression problem to be solved through deep learning algorithms



Deep learning-based internal dosimetry

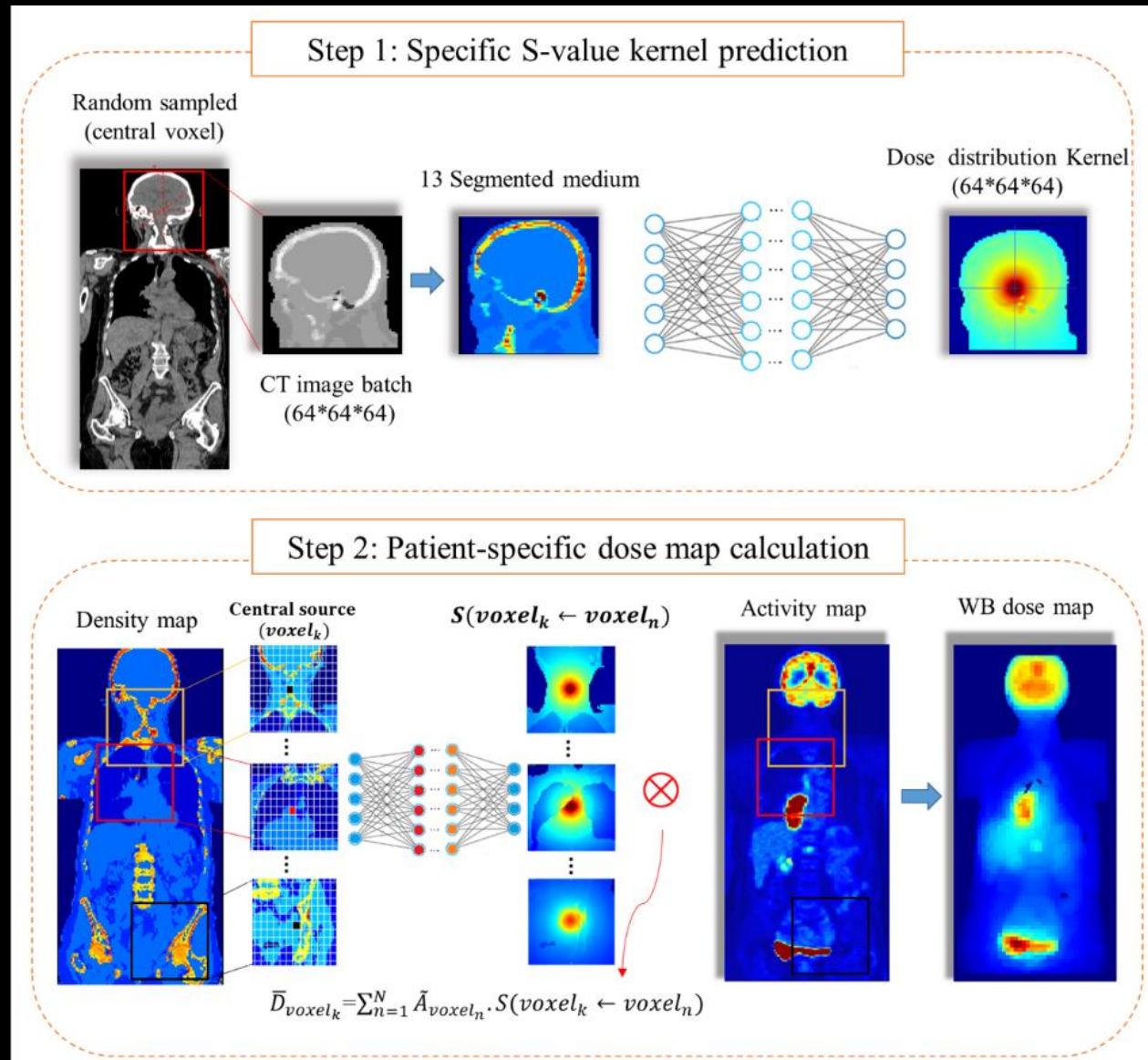


Lee et al. (2018) *Sci Rep*

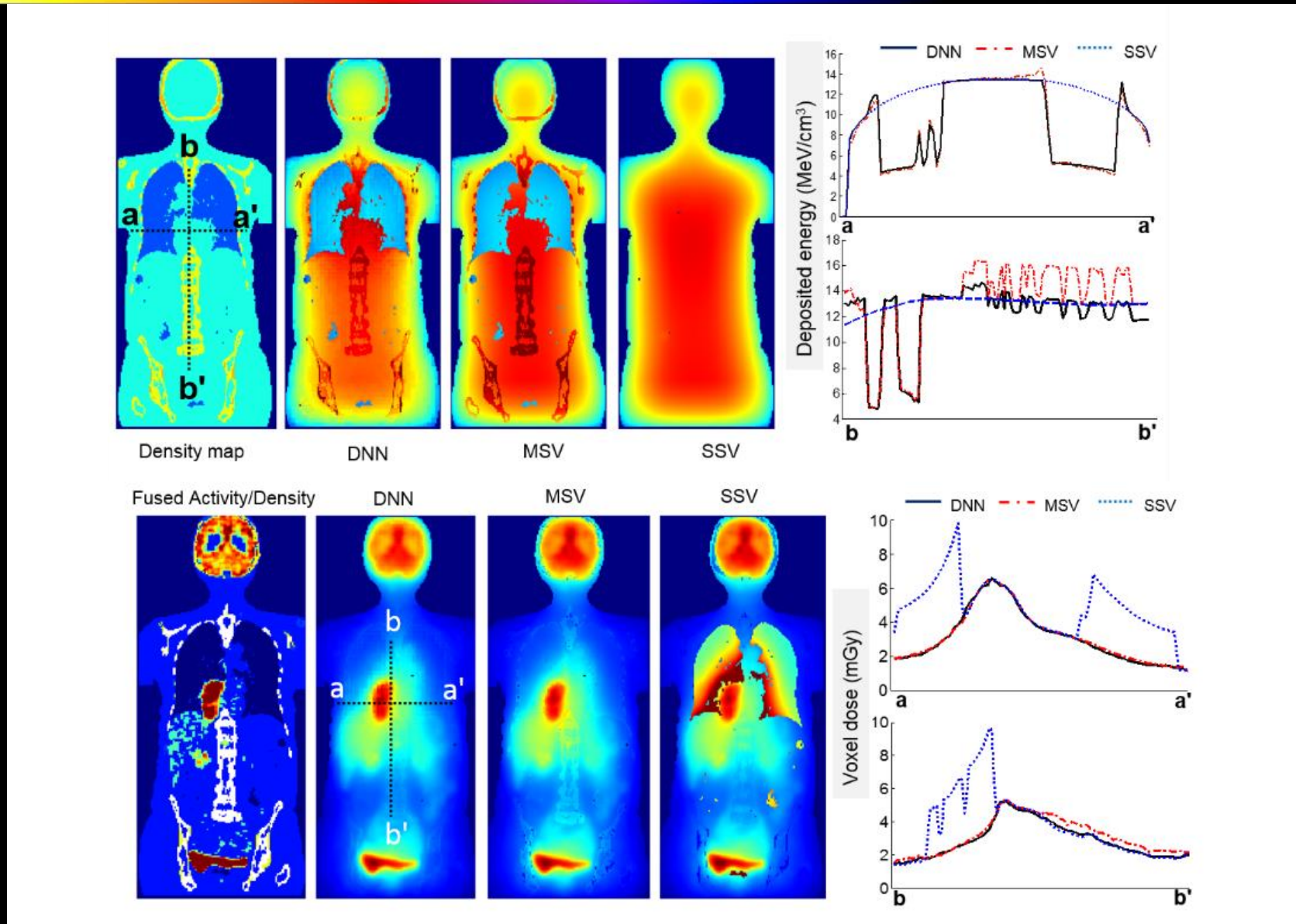


- ✓ SPECT/CT data set of ^{177}Lu -PSMA
- ✓ 2.5D network training (UNet)
- ✓ 2 input channels: MIRD-based dose/CT
- ✓ Output: Whole body dose map

Deep learning-guided internal dosimetry

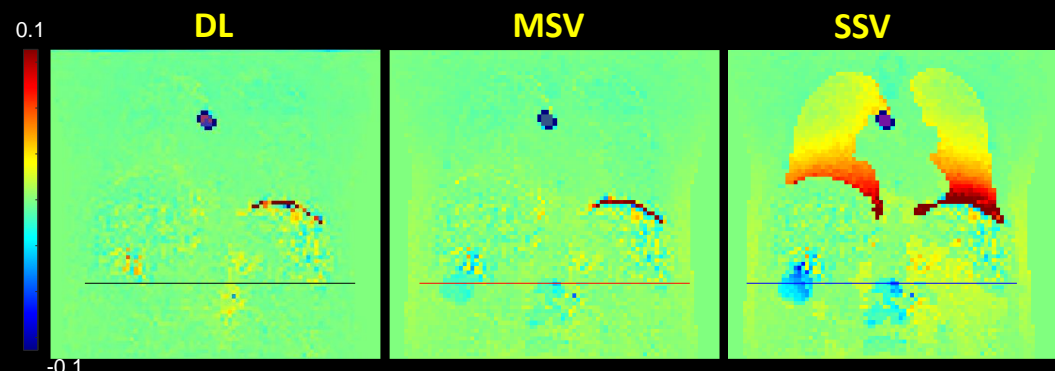
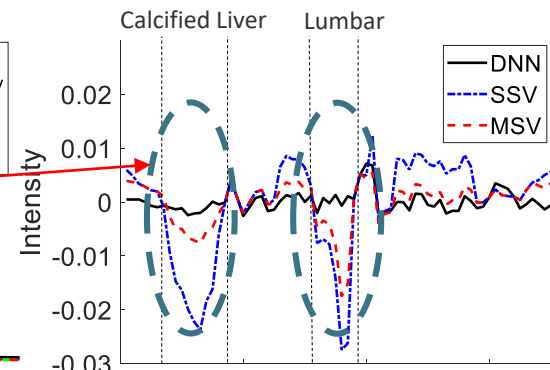
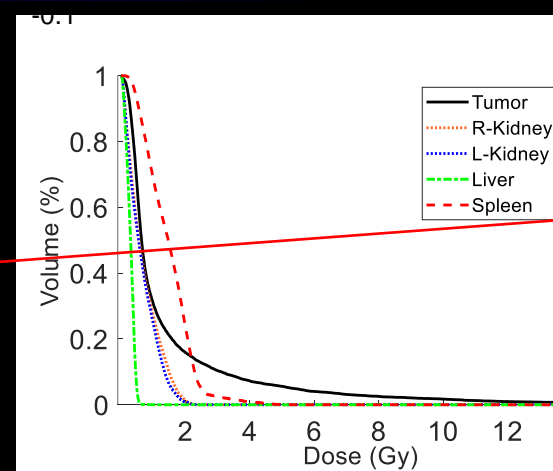
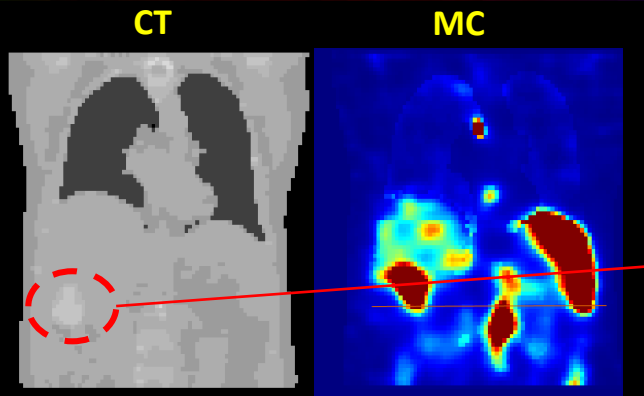


Deep learning-guided internal dosimetry



Deep learning-guided internal dosimetry

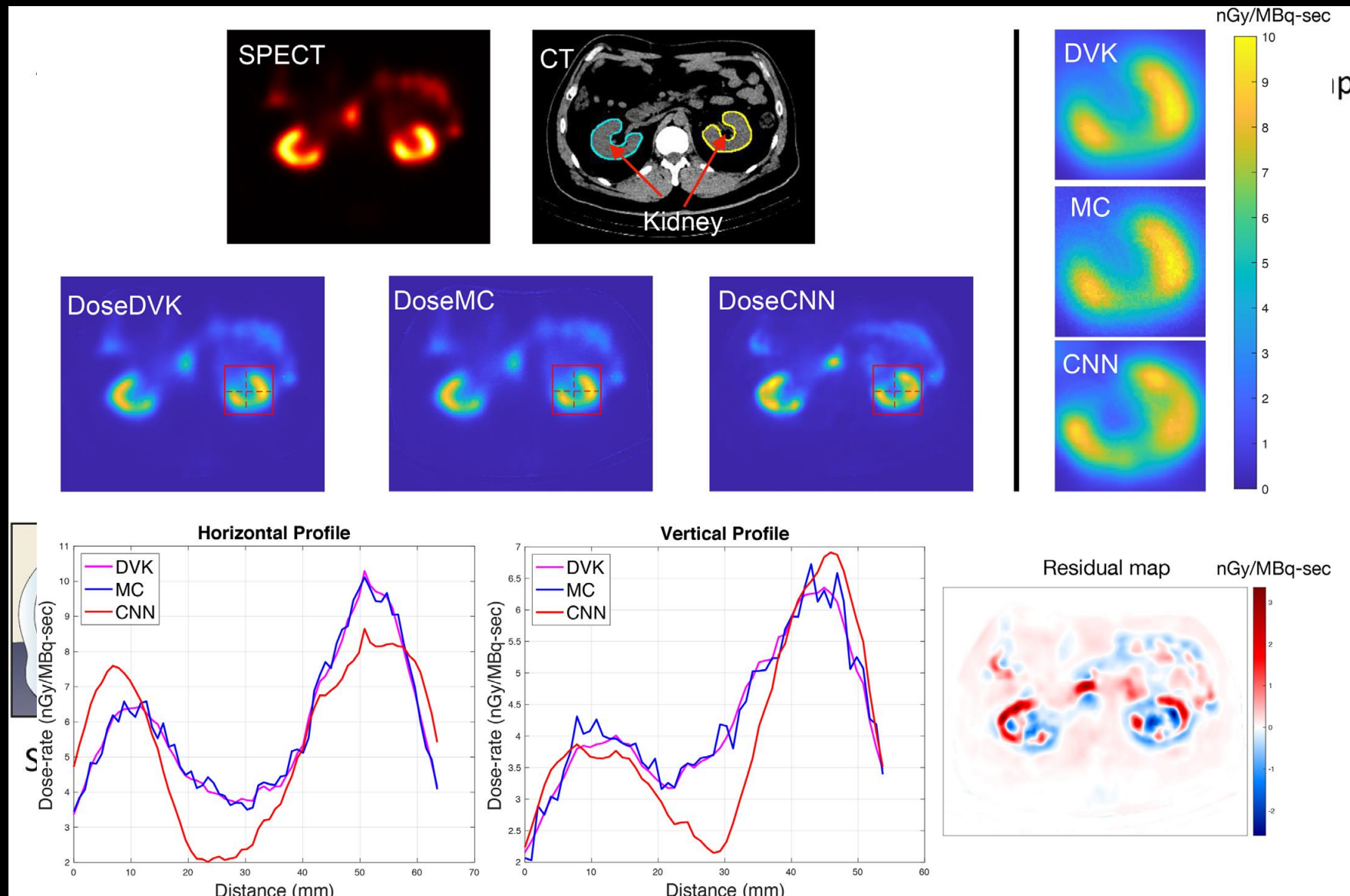
177Lu-Dotatate



Line profile passing through a calcified liver mass

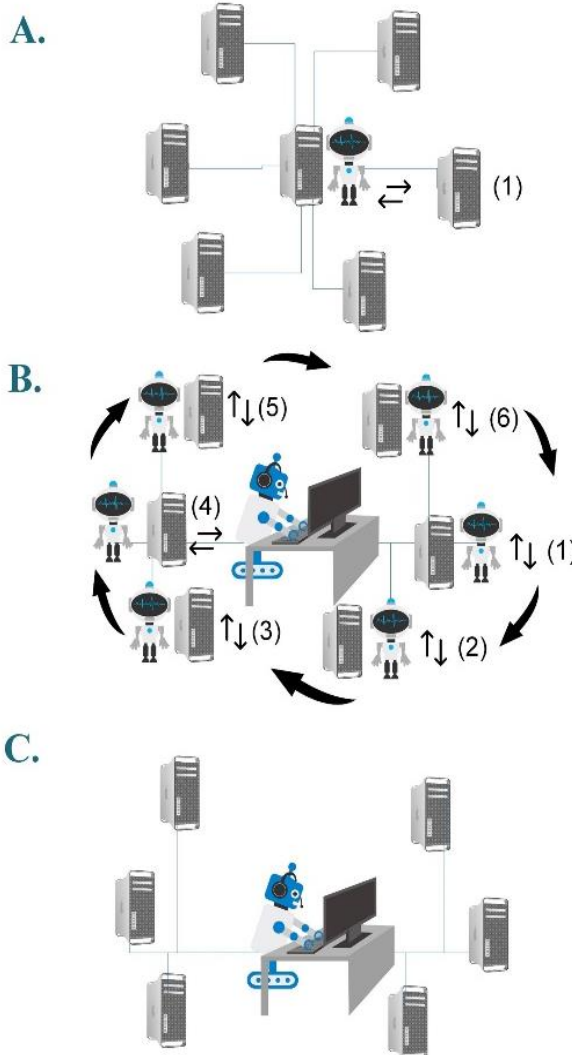
ROIs	MC	DL	MSV	SSV
Tumors	1.38	1.39	1.36	1.36
R-Kidney	0.72	0.72	0.72	0.72
L-Kidney	0.68	0.68	0.68	0.68
Liver	0.31	0.31	0.31	0.31
Spleen	1.49	1.49	1.49	1.50

Deep learning-guided internal dosimetry



Federated learning for PET AC/segmentation

Federated Learning Sequential



300 patients from
6 different centers

Require: num_federated_rounds T

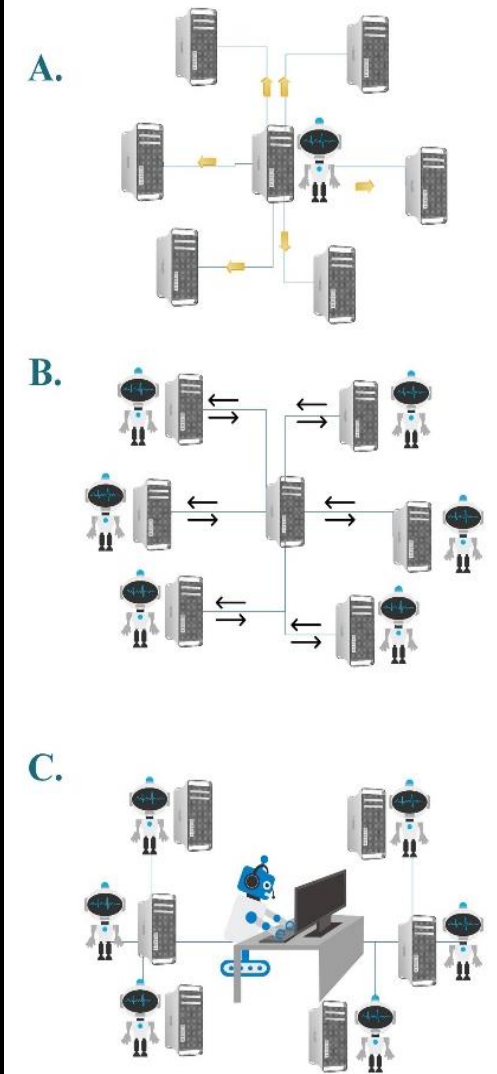
```

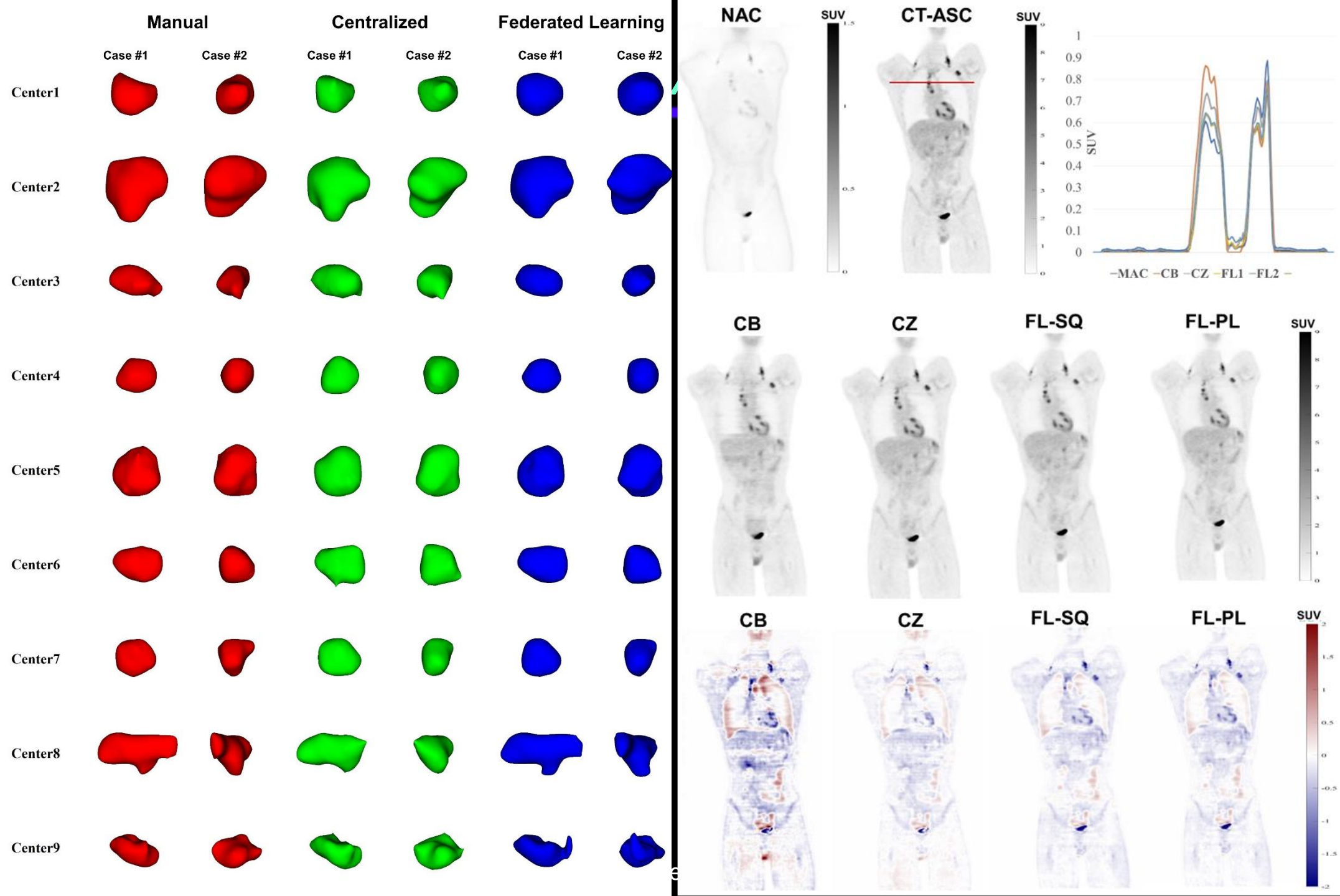
1: procedure AGGREGATING
2: Initialise global model:  $W^{(0)}$ 
3: for  $t \leftarrow 1 \dots T$  do
4:   for client  $k \leftarrow 1 \dots K$  do    > Run in parallel
5:     Send  $W^{(t-1)}$  to client  $k$ 
6:     Receive model updates and number of local training iterations
       ( $\Delta W_k^{(t-1)}, N_k$ ) from client's local training with  $\mathcal{L}_k(X_k; W^{(t-1)})$ 
7:   end for
8:    $W^{(t)} \leftarrow W^{(t-1)} + \frac{1}{\sum_k N_k} \sum_k (N_k \cdot W_k^{(t-1)})$ 
9: end for
10: return  $W^{(t)}$ 
11: end procedure

```

Sequential (**FL-SQ**) and parallel (**FL-PL**) models were compared with **centralized (CZ)** approach (data are pooled to one server), and **center-based (CB)** approach (model built separately)

Federated Learning Parallel





AI faces reproducibility crisis

IN DEPTH | COMPUTER SCIENCE

Artificial intelligence faces reproducibility crisis

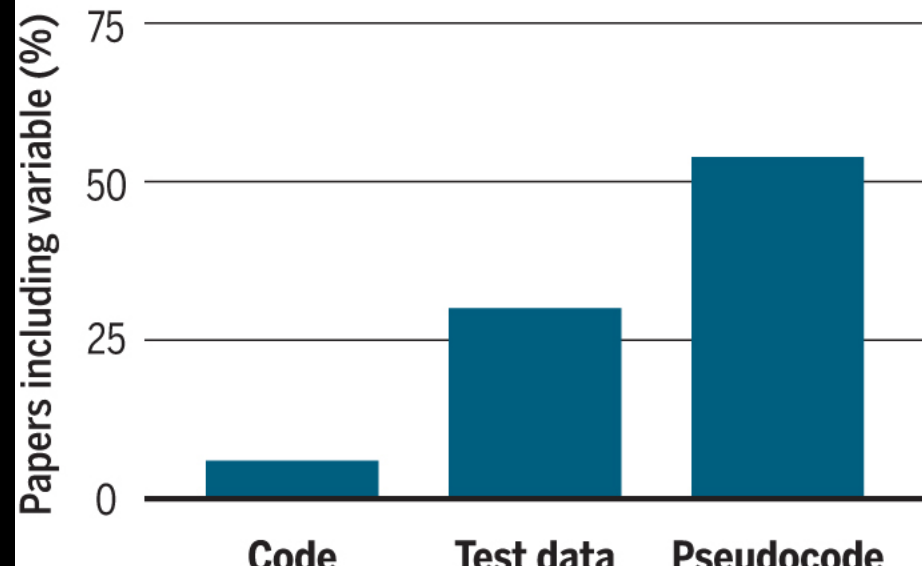
Matthew Hutson

+ See all authors and affiliations

Science 16 Feb 2018:
Vol. 359, Issue 6377, pp. 725-726
DOI: 10.1126/science.359.6377.725

Code break

In a survey of 400 artificial intelligence papers presented at major conferences, just 6% included code for the papers' algorithms. Some 30% included test data, whereas 54% included pseudocode, a limited summary of an algorithm.



Science

Vol 359, Issue 6377
16 February 2018

[Table of Contents](#)
[Print Table of Contents](#)
[Advertising \(PDF\)](#)
[Classified \(PDF\)](#)
[Masthead \(PDF\)](#)

Radiology

COMMUNICATIONS • FROM THE EDITOR

Assessing Radiology Research on Artificial Intelligence: A Brief Guide for Authors, Reviewers, and Readers—From the Radiology Editorial Board

Received: 10 August 2021 | Revised: 10 August 2021 | Accepted: 10 August 2021

DOI: 10.1002/mp.15170

EDITORIAL

MEDICAL PHYSICS

AI in *Medical Physics* Guidelines for publication

Journal of Nuclear Medicine, published on May 26, 2022 as doi:10.2967/jnumed.121.263239

Nuclear Medicine and Artificial Intelligence: Best Practices for Evaluation (the RELAINCE guidelines)

Summary

- Imaging biomarkers are a major component of Big Data driven medical knowledge and decision making
- Nuclear medicine physicians and Radiologists who use AI and deep learning will replace those who don't ...
- AI/deep learning are producing challenges in terms of validation in clinical setting but also plenty of research opportunities.
- Is there a future for AI/deep learning in molecular imaging? YES
- If artificial intelligence is possible, so is artificial stupidity ...
- Wide and specific participation by industry and research communities, planning for long term sustainability

Take home message ...

“Machine learning works very well, and we don’t know why it works so well. I consider that a challenge for mathematicians is to understand it better. I believe if something works, there is a reason. We have to find the reason”

Prof. Ingrid Daubechies, Duke University



Thank you!



This work was supported by the Swiss national Science Foundation (grant 31003A-149957), the Swiss Cancer Research Foundation (grant KFS-3855-02-2016), Eurostars (grants ILLUMINUS E!12326 and Provision E!114021), EEC/H2020 grant NFRP-945196 SINFONIA, Qatar National Research Fund (grant NPRP10-0126-170263) and Fondation privée des HUG (grant RC-06-01).

Thank you!

*Thanks to all my colleagues, too many to mention,
who have participated in the formulation process of
the ideas behind this presentation*

*"Scientists are very happy people
because their job is also their hobby"*

*Prof. Abdus Salem
1979 Nobel Laureate - Physics*

